Reviewed Preprint
v1 • March 4, 2025
Not revised

Reviewed Preprint
v2 • February 17, 2026
Revised by authors

For correspondence:
Philipp.Koch@zi-mannheim.de

* **Author notes:** See page 28

Reviewing editor: Mariano Soiza-Reilly, Universidad de Buenos Aires - CONICET, Argentina

© 2025, Schmidt et al. This article is distributed under the terms of the Creative Commons Attribution License, which permits unrestricted use and redistribution provided that the original author and source are credited.

Psilocin fosters neuroplasticity in iPSC-derived human cortical neurons

Malin Schmidt[1,2,3], Anne Hoffrichter[1,2,3], Mahnaz Davoudi[1,2,3], Sandra Horschitz[1,2,3], Thorsten Lau[1,2,3,4], Marcus W Meinhardt[5,6], Rainer Spanagel[5,7], Julia Ladewig[1,2,3], Georg Köhr[8], Philipp Koch[1,2,3,7]

[1]Department of Translational Brain Research, Central Institute of Mental Health (ZI), University of Heidelberg/ Medical Faculty Mannheim, Mannheim, Germany • [2]Hector Institute for Translational Brain Research (HITBR gGmbH), Mannheim, Germany • [3]German Cancer Research Center (DKFZ), Heidelberg, Germany • [4]Department of Neuroanatomy, Mannheim Centre for Translational Neuroscience (MCTN), Medical Faculty Mannheim, Heidelberg University, Mannheim, Germany • [5]Institute for Psychopharmacology, Central Institute of Mental Health (ZI), University of Heidelberg/ Medical Faculty Mannheim, Mannheim, Germany • [6]Molecular Neuroimaging, Central Institute of Mental Health (ZI), University of Heidelberg/ Medical Faculty Mannheim, Mannheim, Germany • [7]German Center for Mental Health (DZPG), partner site Mannheim-Heidelberg-Ulm, Mannheim, Germany • [8]Department of Neurophysiology, Mannheim Center for Translational Neuroscience (MCTN), University of Heidelberg/Medical Faculty Mannheim, Mannheim, Germany

eLife Assessment

This **fundamental** study reports the effects of the psychedelic drug psilocin on iPSC-derived human cortical neurons, analyzing different aspects of structural and functional neuronal plasticity. The evidence is **convincing** and supports the value of using iPSC-derived human cortical neurons for testing the potentially translational effects of psilocin and other psychedelic-related compounds.

https://doi.org/10.7554/eLife.104006.2.sa3

Abstract

Psilocybin is studied as innovative medication in anxiety, substance abuse and treatment-resistant depression. Animal studies show that psychedelics promote neuronal plasticity by strengthening synaptic responses and protein synthesis. However, the exact molecular and cellular changes induced by psilocybin in the human brain are not known. Here, we treated human cortical neurons derived from induced pluripotent stem cells with the 5-HT2A receptor agonist psilocin - the psychoactive metabolite of psilocybin. We analyzed how exposure to psilocin affects gene expression, neuronal morphology, synaptic markers and neuronal function. Psilocin provoked a 5-HT2A-R-mediated augmentation of BDNF abundance. Transcriptomic profiling identified gene expression signatures priming neurons to neuroplasticity. On a morphological level, psilocin induced enhanced neuronal complexity and increased expression of synaptic proteins, in particular in the postsynaptic-compartment. Consistently, we observed an increased excitability and enhanced synaptic network activity in neurons treated with psilocin. In conclusion, exposure of human neurons to psilocin might induce a state of enhanced neuronal plasticity which could explain why psilocin is beneficial in the treatment of neuropsychiatric disorders where synaptic dysfunctions are discussed.

Introduction

Since the 90's the mind-altering psychedelics have become again the subject of an intriguing stream of research in psychiatric disorders[1,2]. Particularly, in times where the development and the approval of new medications is decreasing and the number of patients suffering from psychiatric disorders is rising there is a huge need for new therapeutical interventions[3,4]. Compared to classical drugs the broad therapeutical effect of psychedelics is rapid, robust and can

be long-lasting even after single administration[5]. In particular, the 5-hydroxytryptamine receptor 2A (5-HT2A-R) targeting psilocybin, the compound of the so-called "magic mushrooms", is discussed as fast-acting and long-lasting antidepressant in treatment-resistant depression (TRD), anxiety, obsessive-compulsive disorder and addiction[6–11]. Not surprisingly psilocybin is stated as "breakthrough therapy" by the United States Food and Drug Administration (FDA) in the treatment of depression since 2019. While we know that 5-HT2A- R activation plays a principal role in serotonergic psychedelic-mediated behavioral and cellular response[12–22] the molecular and cellular changes induced in the brain - on a single cell and network level are barely understood. The recent demonstration of intracellular 5-HT2A-Rs additionally increased the complexity of psychedelic actions[23]. The administration of psychedelics may enable brain network resetting[1] by generating a plastic cellular state in which synaptic remodeling and augmentation of neuroplasticity-associated proteins and genes are likely[24]. Indeed, biological evidence for the "resetting" hypothesis comes from a pioneering study by Olson and colleagues in 2018 which showed that the treatment with serotonergic psychedelics increases the synthesis of synaptic proteins, strengthens synaptic responses, and fosters neurito- and synaptogenesis in rat cortical neurons[25]. The group therefore introduced the term "psychoplastogen" (greek: psych- (mind), -plast (molded), - gen (producing) for underlining their plasticity-promoting properties. Moreover, serotonergic psychedelics already have been shown to promote the 5-HT2A-R-mediated growth of dendritic spines and modulate neurotransmission[25–27]. As molecular and cellular psychedelic research is recently based nearly exclusively on animal studies, the question emerged whether those insights can be translated to the human brain. Psychiatric disorders and psychedelic effects are complex, multisymptomatic and therefore often difficult to study in non-human model organisms. Most importantly, drugs that are efficiently tested in psychiatric animal models might not be necessarily transferable to the human system[28]. In that context, induced human pluripotent stem cells (iPSC) have emerged as a powerful tool to generate neurons and neuronal circuitries, model brain disorders and identify the molecular mechanisms of drug interventions[29].

Here, we explored the molecular, transcriptional, morphometric and functional consequences of the psychoactive 5-HT2A receptor agonist psilocin, the active metabolite of psilocybin in human iPSC- derived cortical neurons. We demonstrate that psilocin leads to a set of molecular, morphological and functional changes that start shortly after administration and manifest in time. These include an increase in brain derived neurotrophic factor (BDNF) expression and an activation of gene expression programs associated with neuromodulation and plasticity resulting in increased neuronal complexity, synaptogenesis and changes in neuronal network function. Thus, our study provides first evidence that the 5-HT2A receptor agonist psilocybin activates widespread neuroplastic programs in human neurons.

Results

Differentiation of human iPSCs in human cortical neurons

As an experimental model to study the effects of psilocin in human neurons and neuronal networks we differentiated human iPSCs (expressing the pluripotency-associated transcription factors OCT4 and SOX2) into neural progenitor cells which we further differentiated into neurons of mainly dorsal forebrain identity (Fig. 1A and Fig. S1A-B)[30–33]. Neural progenitor cells express typical neural stem / progenitor cell markers such as NESTIN or SOX2 as well as the dorsal forebrain-associated transcription factors PAX6 and are negative for FOXA2, as floorplate/ midbrain marker (Fig. S1B). Neurons differentiated from these progenitors for >5 weeks express the neuronal antigen NeuN, the dendritic marker MAP2, and the axonal marker TAU. Most neurons express TBR1 and / or CTIP2, transcription factors typically found in Layer 5/6 neurons of the human cortex (Fig. 1A). Neuronal activity in mature neurons is indicated by expression of the activity-dependent immediate early gene cFOS (Fig. 1A). Astrocytes expressing glial fibrillary acid protein (GFAP) were found occasionally (Fig. 1A). These represent the only contamination in the otherwise purely neuronal culture, which contains no residual progenitors (Fig. S1C). 5-HT2A-R expression was confirmed by PCR (Fig. S1D)[34,35].

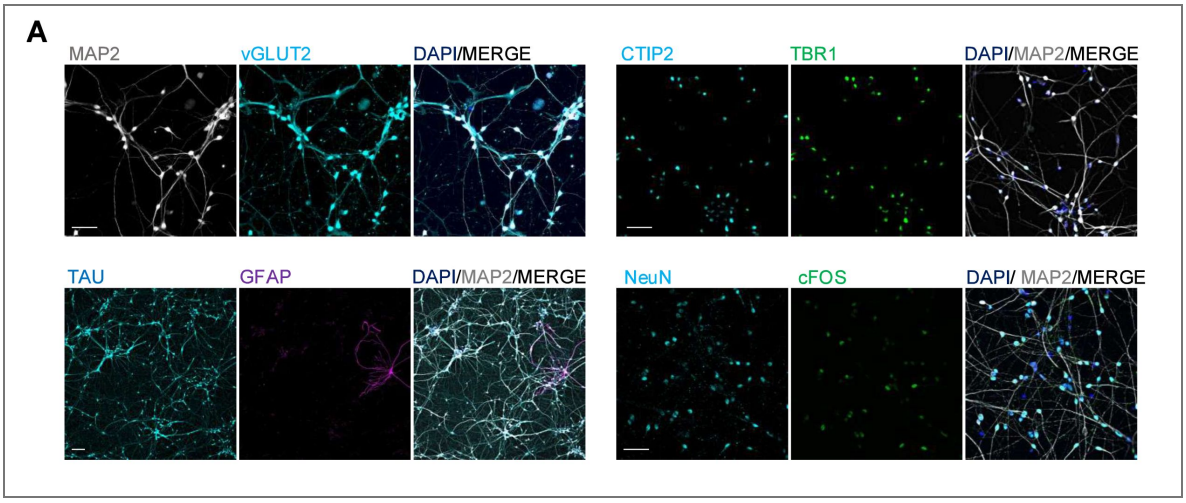

Fig. 1. Validation of mature cortical neuron properties.

(A) hiPSCs were differentiated *in vitro* into glutamatergic cortical neurons over a neuronal progenitor step since the cerebral cortex is a key region for psychedelic effects and psychiatric disorders. Mature 40-day old cortical neurons were glutamatergic (vGLUT2 expression) and expressed cortical layer markers like TBR1, CTIP2 and the neuronal markers NeuN, MAP2 and TAU. cFOS expression is a sign for neuronal activity. GFAP expression indicated a low amount of astrocytes. Scale bar: 50 pm, for GFAP staining 100 pm.

Psilocin induces BDNF expression and downstream signaling in human neurons

Psychedelics have been shown to efficiently increase levels of neurotrophic factors, such as BDNF[12,25,36,37]. We thus addressed BDNF expression in human neurons following exposure to psilocin. We analyzed the effect of different psilocin concentrations (ranging from 10 nM to 10pM) exposed for 10 min and also at 24 hrs following exposure. We observed a dosage-dependent increase in the abundance of BDNF-positive particles (quantified as particles per pm neurite length) which reached significance at a concentration of 10 µM psilocin (Fig. S2A-B). A longer treatment (6 hrs instead of 10 min) with a lower concentration (100 nM instead of 10 pM) of psilocin also induced BDNF abundance significantly, but less strikingly (Fig. S2C-D). We thus continued to use 10 µM psilocin in the following experiments. The clear induction of BDNF particle density was reproduced in four biological independent control cell lines and several differentiation batches for each line (from MCtrl = 1.5 ± 1.2; MPsi = 2.6 ± 1.9) (Fig. 2A-C). When comparing BDNF densities independently in dendrites (MAP2-positive) and axons (Tau-positive), the significant increase in BDNF could be assigned to both neuronal compartments to a comparable extent (Fig. S2E-F). Also, at 48 hrs following the exposure to psilocin, a significant increase of BDNF particles was observed compared to the untreated condition (Fig. S2G). The increase in BDNF abundance was 5-HT2A-R-mediated as treatment of the neurons with the specific 5-HTR2A-R antagonist ketanserin prevented BDNF upregulation by psilocin (Fig. 2D-E) (from MCtrl = 1.8 ± 0.8; MPsi = 3.4 ± 1.7; MPsi + Ket = 1.5 ± 0.7; MKet = 1.4 ± 1.2). Upregulation of BDNF could also be prevented by blocking CME with dynasore or protein kinase C (PKC) with the PKC inhibitor chelerythrine, indicating that CME and PKC activation are critically involved in this process (Fig. 2F-G) (from MCtrl= 3.1 ± 1.5 to MPsi = 4.6 ± 2.4; MPsi + Chel = 3 ± 1.7; MPsi + D = 3.4 ± 1). Upregulation of BDNF was also validated by Western immunoblot where we observed an increase in the levels of pro- BDNF and were able to detect mature BDNF at approximately 14 kDa, which, under baseline conditions, was below the detection level (Fig. S2H). Increased BDNF signaling in psilocin-treated neurons is indicated by an increase in the phosphorylation of the BDNF receptor TrkB (Fig. S2H). Furthermore, as a downstream target of BDNF signaling we observed an increase of the phosphorylation of AKT at Ser 473 1 day (Fig. S2I) and 3 days after psilocin exposure (Fig. 2H-I) which was reversed by ketanserin treatment (from MCtrl = 0.8 ± 0.2; MPsi = 1.3 ± 0.2; MKet = 0.9 ± 0.2).

Psilocin induces gene expression changes associated with axonal and synaptic plasticity

To analyze the influence of psilocin on global gene expression in cortical neurons, we performed whole transcriptome sequencing one day and three days following a single 10 min administration with 10 µM psilocin in neurons from two independent genetic backgrounds. GO enrichment and KEGG pathway analysis comparing cells one day and three days after psilocin administration with the respective controls revealed an enrichment of significantly affected genes in many ontologies and pathways associated with axonal growth and synaptic remodeling, plasticity and learning, memory and cognition (Fig. 3A, S3A). Most significant changes occurred within the first 24 hrs which is reflected when plotting the significantly changed genes only for selected GO term enriched at both time points (Fig. 3B, S3B). When looking at a more global gene expression level of all genes included in the respective GOs, gene expression of GOs associated with axonal outgrowth show a generally higher expression at day 1 which is further increased at day 3. In contrast genes associated to synaptic organization, plasticity and learning, memory and cognition show a trend towards decreased expression at day 1 and a generally stronger increase at day 3 (Fig. 3C, S3C). The overlapping assignment of significant differentially expressed genes to the aforementioned GOs underlines their importance in long-term plasticity (e.g., *CDK5*, *CAMK)*, synapse formation (e.g., *SYN1*) and axonal and neurite growth (e.g., *GAP43*) and neuronal structure marker (e.g., *MAPT)* (Fig. 3D). The latter is consistent with increasing staining intensity for TAU (Fig. 2). We further found a strong significant upregulation of immediate early genes

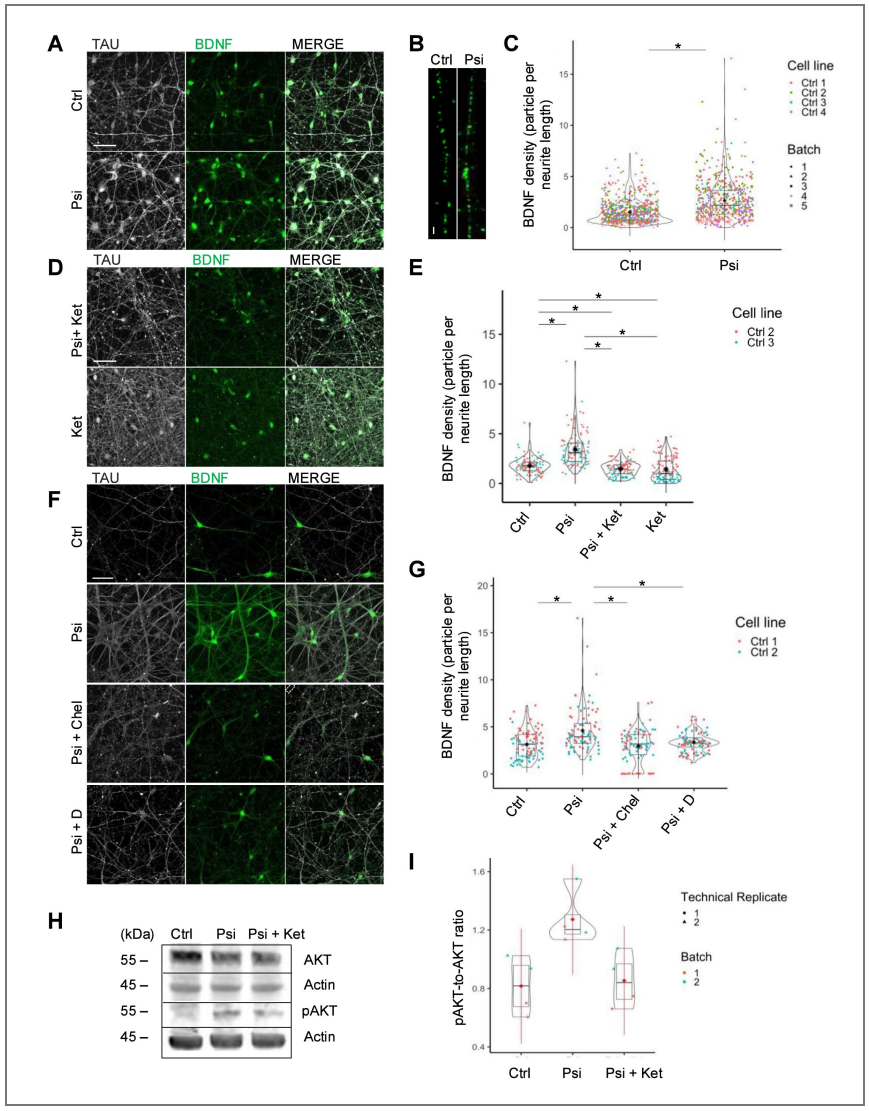

Fig. 2. Psilocin-induced increase in BDNF level was 5-HT2A receptor and PKC- and endocytosis mediated and induced activation of m-BDNF/TrkB-associated downstream pathway.

(A-B) Representative image of a neuronal network for pre-treatment condition (Ctrl) and 24 hrs after a 10 min 10 µM short psilocin trigger (Psi). Scale bar: 50 pm, (B) close up: 2 pm. (C) BDNF density was significantly increased 24 hrs after a 10 min 10 µM psilocin trigger (Psi). Four Ctrl cell lines were included in the analysis (Ctrl with N = 613 neurites; Psi with N = 529 neurites). (D) Representative image 24 hrs after the simultaneous treatment with psilocin and ketanserin (Psi + Ket) and single treatment with ketanserin (Ket), scale bar: 50 pm. (E) Ketanserin co-treatment (Psi + Ket) and ketanserin monotreatment (Ket) significantly reduced BDNF density compared to the 24 hrs monotreatment psilocin condition, suggesting a 5-HT2A-mediated process. Ketanserin monotreatment provoked a significant reduction in BDNF density compared to ketanserin co-treatment with psilocin. Two Ctrl cell lines were included in the analysis, each with one biological batch (Ctrl with N = 99 neurites; Psi with N = 102 neurites; Psi + Ket with N = 102 neurites; Ket with N = 102 neurites). (F) Representative image 24 hrs after the simultaneous treatment of 10 µM psilocin with chelerythrine (Psi + Chel) or dynasore (Psi + D), scale bar: 50 pm. (G) Chelerythrine (Psi + Chel, selective PKC inhibitor) or dynasore (Psi + D, inhibition of clathrin-coated vesicle invagination) co-treatment significantly reduced BDNF density compared to the psilocin monotreatment condition (Psi). Two Ctrl cell lines were included in the analysis, each with one biological batch (Ctrl with N = 90 neurites; Psi with N = 90 neurites; Psi + Chel with N = 90; Psi + D with N = 90 neurites). (H) Phosphorylated AKT (pAKT) protein level was increased 72 hrs after psilocin exposure (Psi), reversed by ketanserin co-treatment (Psi + Ket), (I) both effects were not significant. Ctrl cell line 3 was included in the analysis (Ctrl with N = 4 data points, Psi with N = 4 data points, Psi + Ket with N = 4 data points), each with two biological batches. For all analyses Kruskal-Wallis-Test for independent samples was calculated. Post hoc Wilcoxon rank sum test. Bonferroni-correction, adjusted $p < .05$, mean ± SD. Significance levels against the respective control and for multiple group comparisons are *$p < .05$.

(lEGs) (e.g., *FOSL2*, *JUND*, *EGR1*, *ARC*, *FOSB*) and of the excitatory glutamatergic AMPA/NMDA receptor genes (*GRIA/GRIN*) after psilocin administration (Fig. 3E). One day but not three days of psilocin treatment more strongly upregulated the AMPA genes *GRIA1, 2, 3* than the NMDA genes *GRIN1, 2B, 2C* (Fig. 3E), supporting modulation of glutamatergic excitatory signalling genes upon psilocin treatment. These effects could be reversed upon co-treatment with antagonist ketanserin, indicating that most changes are 5-HT2A receptor mediated (Fig. 3F).

Psilocin increases neurite complexity

The gene expression analysis indicated an induction of morphometric changes by psilocin in particular on neurites. Therefore, we assessed neuronal complexity performing Sholl analysis in neurons differentiated for >40 days at 24 hrs and 48 hrs following psilocin exposure. To identify the dendritic arbor of single mature neurons in these cultures, the cultures were transduced with adeno-associated vectors (AAVs) coding for mCherry under control of the CaMKIIa promoter (Fig. 4A-D).

We observed an increase of primary neurites at 25 µm (significant at 48 hrs and a trend at 24 hrs from MCtrl = 4.1 ± 2.1; M24hrs = 5.4 ± 3.7; M48hrs = 5.5 ± 2.4) and of intersections at 50 µm (significantly increased at 24 and 48 hrs post treatment from MCtrl = 2.7 ± 1.4; M24hrs = 4 ± 2.3 to M48hrs = 3.9 ± 1.8; Fig. 4B). As a result, the calculated total neurite length was significantly increased at 24 and 48 hrs post treatment from MCtrl = 272.5 ± 142.7; M24hrs = 383.2 ± 209.9; M48hrs = 352.8 ± 162.5 (Fig. 4C). And we observed a significant increase in the total number of intersections in psilocin-exposed neurons quantified in steps of 25 µm up to a distance of 125 µm (MCtrl = 10.9 ± 5.7; M24hrs = 15.3 ± 8.4, M48hrs = 14.1 ± 6.5; Fig. 4D). These data indicate, that gene expression changes elicited by psilocin resulted in neurite outgrowth and an increase of global dendritic complexity as early as 24h following a single 10 min exposure.

Psilocin increases synaptic strength and synaptogenesis

To address changes on neuronal function, we exposed neuronal cultures 10 min or 24 h to 10 µM psilocin and performed whole-cell patch-clamp experiments one week later. Following the 10 min exposure, we observed a increasing trend in the number of evoked action potentials (APs), having amplitudes of around 100 mV (Fig. 5A). Extended exposure of the cultures to psilocin (24h) increased this effect reaching significance (total number of APs from MCtrl = 20.1 ± 12; MPsi 10min; day 7 = 28.9 ± 16.9; MPsi 24hrs; day 7 = 30 ± 14.5; AP amplitude from MCtrl = 101.1 ± 13.3; MPsi 10min; day 7 = 101.1 ± 13.2; MPsi 24hrs; day 7 = 101.3 ± 16.7). To find out whether the increase in AP firing enhanced synaptic network activity, we recorded spontaneous AP-dependent excitatory postsynaptic currents (sEPSCs). Indeed, the frequency of sEPSCs increased in both psilocin-treated conditions to some extent (MCtrl = 0.6 ± 0.7; MPsi 10min; day 7 = 1.0 ± 1.3; MPsi 24hrs; day 7 = 1.1 ± 1.2; Fig. 5B). And, we observed a slight increase in sEPSC amplitude (MCtrl = 14.2 ± 4.7; MPsi 10min; day 7 = 16.7 ± 5.1; MPsi 24hrs; day 7 = 15.5 ± 5.3; Fig. 5B), consistent with the observed *GRIA* upregulation (Fig. 3E). The latter amplitude increase was next examined on AP-independent miniature EPSCs (mEPSCs) which are generally caused by the spontaneous release of single vesicles (Figs. 5C, S4A). The amplitudes of mEPSCs increased 7 days after the start of 24 hrs psilocin administration consistently for two cell lines (MCtrl = 11.1 ± 2.2; MPsi 24hrs; day 7 = 12.8 ± 4.2, Fig. 5C; MCtrl = 9.3 ± 2.8; MPsi 24hrs; day 7 = 11.2 ± 3.7, Fig. S4A), whereas the frequencies of the mEPSCs were rather stable (MCtrl = 0.8 ± 0.5; MPsi 24hrs; day 7 = 0.9 ± 0.6, Fig. 5C; MCtrl = 0.9 ± 0.7; MPsi 24hrs; day 7 = 0.7 ± 0.5, Fig. S4A). When examining mEPSCs from separately differentiated neurons exposed to psilocin for 24 hrs and analyzed at day 11, the increase in mEPSC amplitude was somewhat attenuated compared with 7 days (MCtrl = 11.7 ± 4.3; MPsi 24hrs; day 11 = 12.4 ± 3.6; frequency from MCtrl = 0.8 ± 0.8; MPsi 24hrs; day 11 = 0.5 ± 0.3, Fig. 5C). Repeated LSD administration altered gene and protein expression related to neuroplasticity signaling in the mouse prefrontal cortex and increased dendritic spine density[38,39]. We therefore hypothesized that extended psilocin administration fosters synaptic network activity and synaptogenesis and thus examined effects of a 96 hrs exposure. In line with the above-mentioned hypothesis, the amplitudes of the sEPSCs increased significantly in two lines (MCtrl = 22.5 ± 6.5;

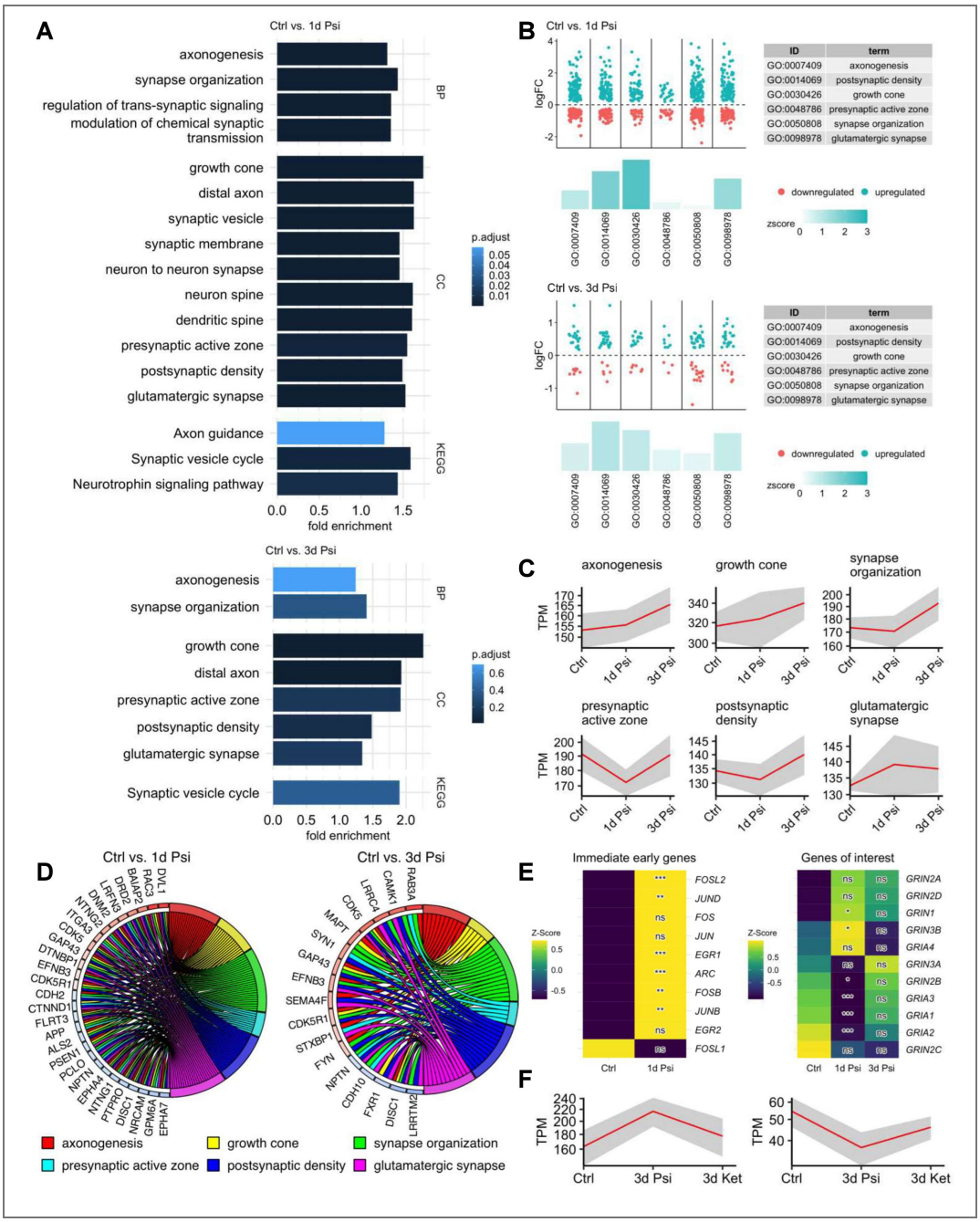

Fig. 3. Psilocin displays fast and enduring changes of the genetic landscape.

(A) Enrichment in differentially expressed genes associated with synapse formation, neuronal plasticity and axonogenesis GO terms 1 day after psilocin administration, and the effect 3 days later. (B) Psilocin induced within 24 hours a first wave of upregulation of selected GO genes based on DESeq2 normalized counts. Log2fold changes of each differentially expressed genes between two conditions are shown as dots. Zscores indicate if more genes in the respective GO term are upregulated or downregulated also indicated by height and color of the bars (C) TPM-normalized mean (red line) of psilocin-induced temporal expression pattern of genes belonging to the indicated GO. Shaded area is indicating SD. (D) Chord plots showing significant genes appearing in at least 4 GO terms (of 6 selected GO terms) 1 day after psilocin administration and appearing in at least 3 GO terms 3 days after psilocin administration. (E). Heat map (z-scaled normalized counts) showing expression of immediate early genes and AMPA/ NMDA receptor genes throughout psilocin administration. (F) Differentially expressed genes, that are up-/ downregulated upon psilocin treatment, showed a reversed effect upon co-treatment with ketanserin. Mean TPM-normalized expression values are shown (red line), shaded area indicates S.D. BP, biological process; CC, Cellular Compartment; KEGG, Kyoto Encyclopedia of Genes and Genomes. TPM, transcripts per kilobase million. Significance levels against the respective control ns: p-adj. > .05, *: p-adj. <= .05, **: p-adj. <= .01, ***: p-adj. <= .001.

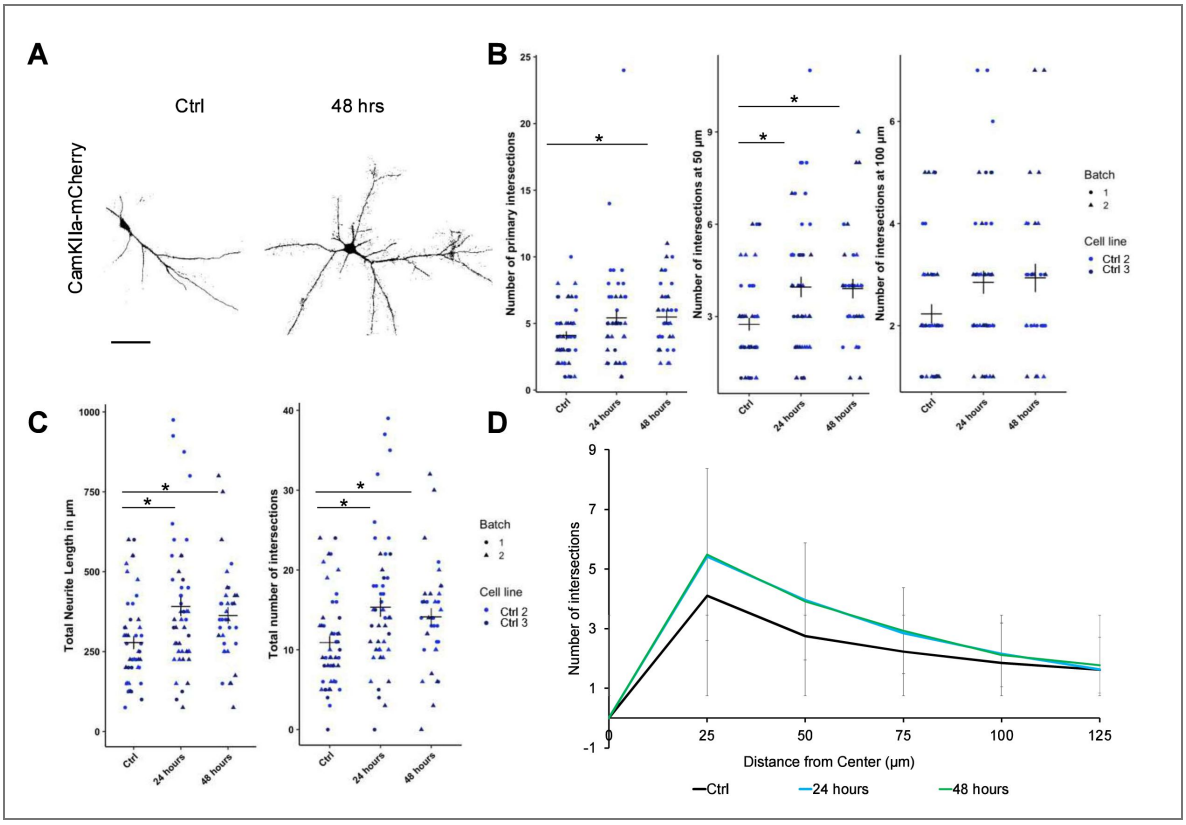

Fig. 4. Psilocin induced neurite branching.

(A-C) Cells were transduced with AAV CamKIIa p-hCHR2(134a)-mCherry. (A) Representative image for pre-treatment condition (Ctrl) and 48 hrs after a 10 min short psilocin trigger (48 hrs) for mCherry staining showed an increase in neurite intersections for the latter. (B) Singular analysis: 48 hrs after a 10 min 10 µM psilocin trigger the number of primary (25 µm distance from soma) neurite intersections significantly increased compared to the untreated control condition (Ctrl). The number of intersections at 50 µm distance from soma significantly increased 24 hrs and 48 hrs after a 10 min 10 µM psilocin trigger. (C) Significant changes for the calculated total neurite length and for the total number of neurite intersections significantly increased 24 hrs and 48 hrs after a 10 min 10 µM psilocin trigger. Two Control cell lines with two biological batches (Ctrl with N = 43 - 48 neurites; 24 hrs with N = 47 - 48 neurites; 48 hrs with N = 31 - 35 neurites) were included. (D) Sholl analyses summary for results shown in figure (B). For all analyses Kruskal-Wallis-Test for independent samples was calculated. Post hoc Wilcoxon rank sum test. Bonferroni-correction, adjusted $p < .05$, mean ± SD. Significance levels against the respective control are *$p < .05$.

MPsi 96hrs; day 10 = 30.7 ± 4.8, Fig. 5D; MCtrl = 15.9 ± 4.5 ; MPsi 96hrs; day 10 = 27.6 ± 10, Fig. S4B), and the frequencies showed a trend to increase similar to Fig. 5B, reflecting enhanced network activity (MCtrl = 1.0 ± 1.0; MPsi 96hrs; day 10 = 1.5 ± 1.0, Fig. 5E; MCtrl = 1.5 ± 1.7; MPsi 96hrs; day 10 = 1.0 ± 0.7, Fig. S4B).

This enhanced synaptic network activity should affect the abundance of either the presynaptic marker synapsin and/or the postsynaptic marker PSD-95 and may even affect their co-localization at day 4 and at day 10 following 4 day permanent 10 µM psilocin administration. In line with above electrophysiological results for the 10 day psilocin exposure (Fig. 5D) and the gene expression data, which indicated changes associated with synaptogenesis and synaptic plasticity (Fig. 3) we observed for the pre-synaptic marker synapsin, a trend towards an increase of the density (particles per neurite length) (from MCtrl = 0.25 ± 0.2; M4days = 0.28 ± 0.2; M10days = 0.29 ± 0.2) and intensity (mean fluorescence intensity of the particles) (from MCtrl = 21 ± 13.3; M4days = 24.1± 15; M10days = 19.8 ±10.9) at both time points (Fig. 5E-H). In line with the gene expression data (Fig. 3A, postsynaptic density), we observed a significant increase in the density of the postsynaptic marker PSD-95 (from MCtrl = 1.1 ± 0.5; M4days = 1.4 ± 0.6; M10days = 1.3 ± 0.5) and in its intensity (from MCtrl = 31.8 ± 12,9; M4days = 36.8 ± 15.6; M10days = 38 ± 16.4) for both time points (Fig. 5I-J). These effects were accompanied by a significant increase in the co-localization of both markers (from MCtrl = 0.2 ± 0.2; M4days = 0.3 ± 0.2; M10days = 0.3 ± 0.2; Fig. 5K). Together, these experiments indicate that psilocin augments synaptic strength primarily via an increase in the postsynaptic receptor density, which lasts at least for 6 days from the start of psilocin withdrawal and that extended exposure of neurons to psilocin pronounces the effects on synaptic strength.

Discussion

The neuroplasticity-promoting psychoplastogen[25] psilocybin is currently developed as a new medication in the treatment of psychiatric disorders[1,2,40]. “Brain network resetting”[1] by psilocybin , i.e. the restoration of neuronal and synaptic dysfunction associated with the pathophysiology of mental disorders[41–45], could be achieved by stimulating signaling pathways associated with neuroplasticity and BDNF signaling[24,41]. So far, experimental evidence for this hypothesis is based on data from non-human model organisms.

In our experimental setting, we observed a pronounced psilocin-induced BDNF upregulation in human cortical neurons and show that PKC activation and endocytosis, two mechanisms contributing to 5- HT2A-R internalization[42,43], are involved as chelerythrine and dynasore inhibited BDNF augmentation. BDNF plays an important role in neurogenesis, synaptogenesis, and the formation of synaptic interactions the basis of neuroplasticity (Fig. S5), the brain’s enduring ability to constantly change in response to influences and experiences and lifelong learning[44]. Particularly the mature BDNF/phosphorylated-TrkB receptor complex is involved in multiple pathways linked to prosurvival and synaptic plasticity[44]. Recently it was shown that psychedelics also directly bind to the BDNF TrKB receptor, thereby affecting TrkB dimerization and facilitating the effect of endogenous BDNF, which underlines the importance of the BDNF system for the action of psychedelics[45]. In keeping with this, we show that psilocin leads to a fast and enduring upregulation of proteins and genes linked to neuronal complexity, synaptogenesis and synaptic transmission, as also demonstrated in psychedelic-mediated plasticity in animal studies[25,26,46]. Of note, BDNF upregulation and changes in gene expression were reversed by ketanserin confirming that these effects are mediated by 5-HT2A-Rs.

In our model, augmentation of neuronal complexity is an outcome which can be detected as early as 24 hrs after psilocin administration. In rodents, serotonergic psychedelics also foster synaptogenesis and spinogenesis[25,26,46]. In line with this we show that psilocin also promotes synaptogenesis, measured by the increase in PSD-95, synapsin and their colocalization. As a result, we observe changes in intrinsic neuronal properties and network function. More specifically, we see an increased excitability and an increase in postsynaptic current frequency but in particular amplitude. The higher number of action potentials generated by current injections could be due to increased dendritic excitability as reviewed by Kwan and colleagues[41]. The increase in synaptic

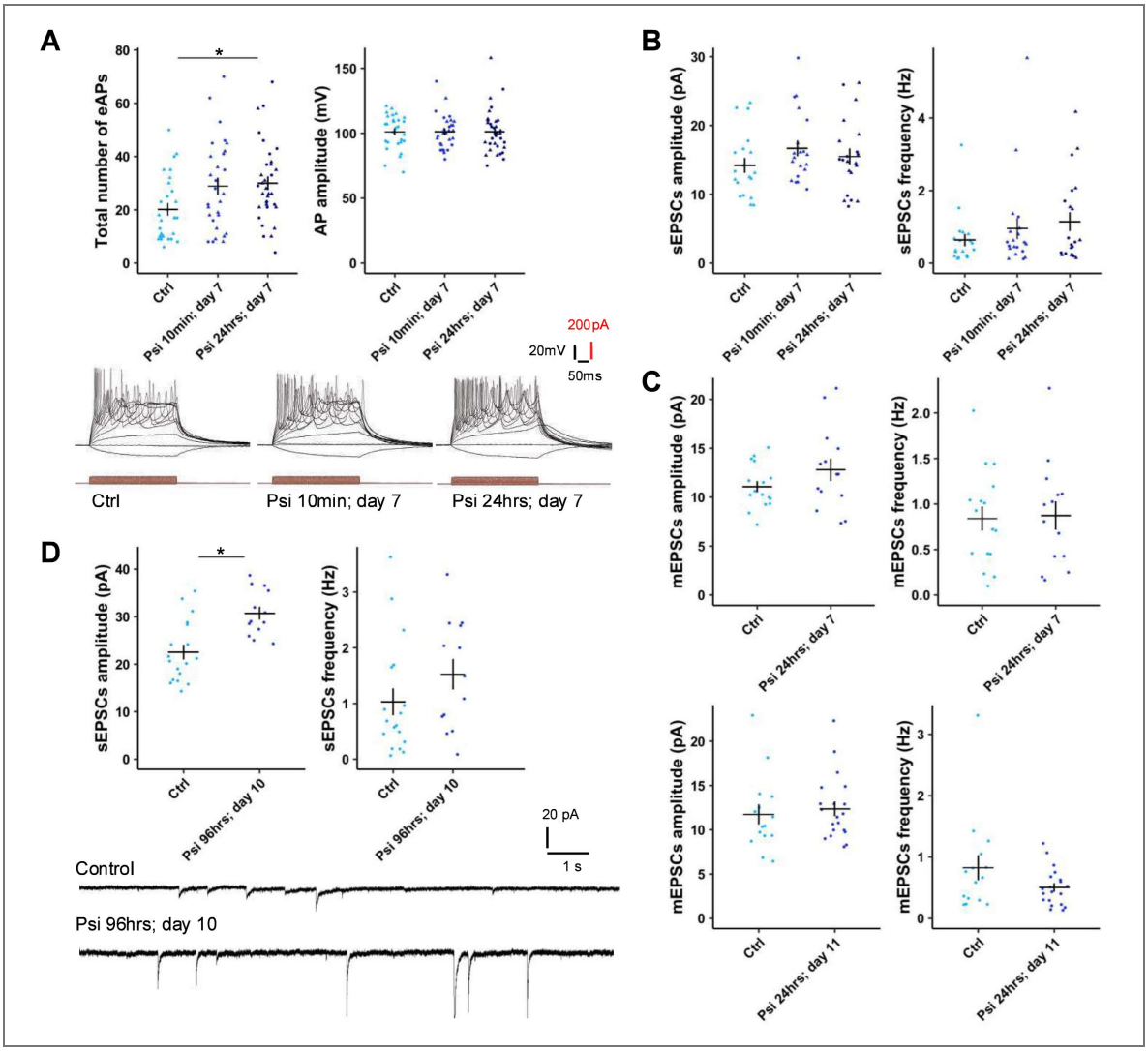

Fig. 5. Psilocin-induced increase in synaptic strength and synaptogenesis.

(A) Total number of evoked action potentials (eAPs) significantly increased at day 7 after 24hrs permanent psilocin administration (Psi 24hrs; day 7) and was increased 7 days after a 10 minutes psilocin trigger (Psi 10min; day 7). AP amplitudes stayed constant. Representative traces for total number of APs. One Ctrl cell line with 2 biological batches was included in the analysis. Ctrl 3 with N = 28 cells, Psi 10min; day 7 with N = 29 cells, Psi 24hrs; day 7 with N = 34 cells. (B) Increase in sEPSCs amplitude and frequency 7 days after 10 minutes and 24hrs permanent psilocin administration. One Ctrl cell line with 2 biological batches was included in the analysis, Ctrl 3 with N = 19 cells, Psi 10min; day 7 with N = 20 cells, Psi 24hrs; day 7 with N = 21 cells. (C) Increase in mEPSCs amplitude 6 days after permanent 10 µM psilocin administration, Ctrl 3 with N = 16 cells, Psi 24hrs; day 7 with N = 14 cells. Increase in mEPSCs amplitude 10 days after 24hrs permanent psilocin administration, Ctrl 3 with N = 15 cells, Psi 24hrs; day 11 with N = 20 cells. (D) Significant increase in sEPSCs amplitude 6 days after 96hrs permanent 10 µM psilocin administration (Psi 96hrs; day 10). Ctrl 3 with N = 18 cells, Psi 96hrs; day 10 with N = 13 cells. Representative traces for control and psilocin condition. For all experiments Mann-Whitney-U-test for independent samples was calculated, mean ± SEM. Significance levels against the respective control are *p < .05. (E-F) Representative dendritic PSD-95 and synapsin staining for the untreated condition (Ctrl), 4 days after permanent 10 µM psilocin administration (4 days) and 10 days after 4 days permanent 10 µM psilocin administration (10 days). (E) Scale bar: 50 µm (F), closeup: 10 pm. Trend in synapsin (G) density and (H) intensity increase 4 days after permanent psilocin administration. (I) PSD-95 particle per neurite length and (J) intensity per area and (K) synapsin/ PSD- 95 co-localization were significantly increased 4 and 10 days after 4 days permanent 10 µM psilocin treatment compared to an untreated control condition. (G-K) Ctrl with N = 180 neurites, 4 days with N = 180 neurites, 10 days with N = 180 neurites. Two control cell lines each with two biological batches were included. For all analyses Kruskal-Wallis-Test for independent samples was calculated. Bonferroni-correction, adjusted p < .05, mean ± SD. Significance levels against the respective control are *p < .05.

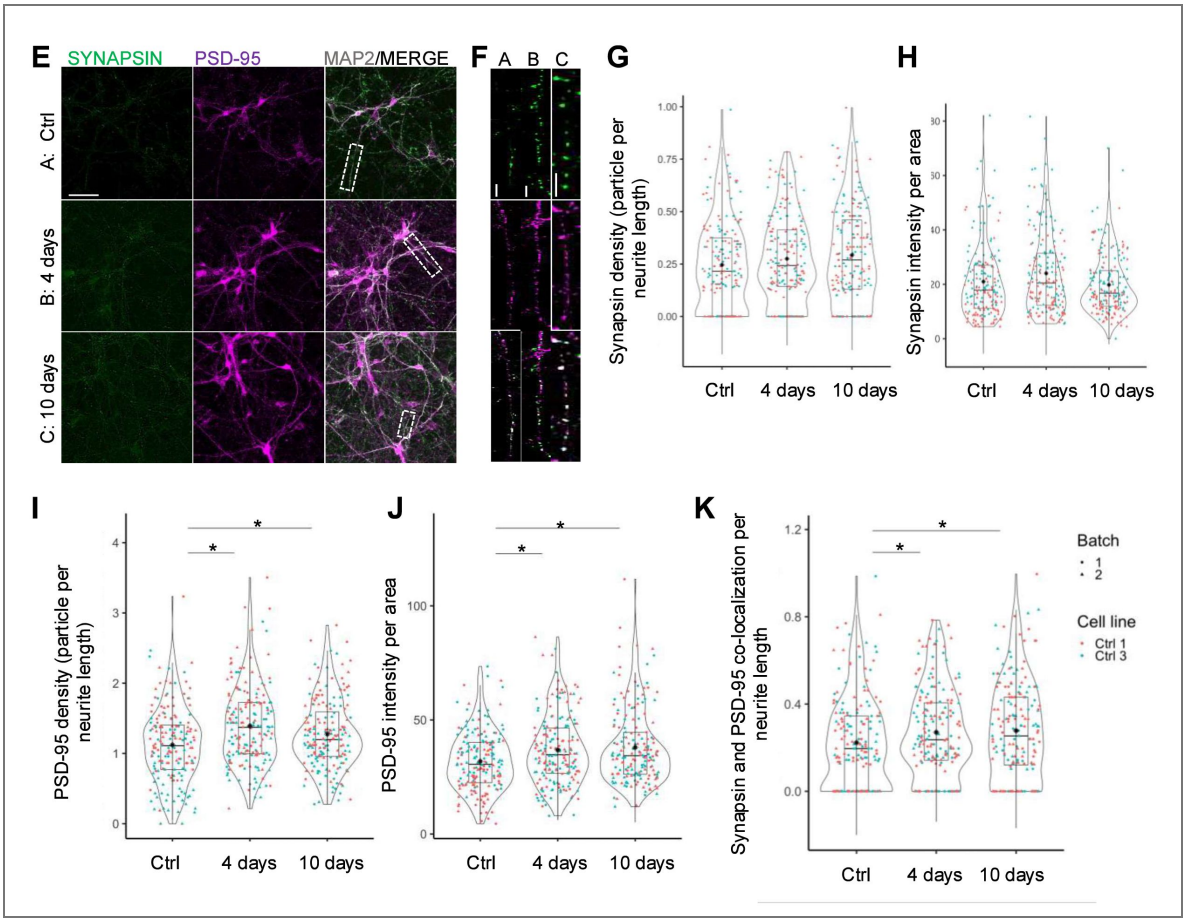

Fig. 5. (continued)

strength lasted at least 6 days and is in agreement with frequency and amplitude increases of miniature and spontaneous synaptic currents observed in acute brain slices of mice after administering psilocybin or DMT *in vivo*[25,26]. These drugs may increase extracellular glutamate levels, similar to ketamine, LSD and DOI administration[24,47–50]. To close the circle, 5-HT2A-R stimulation, subsequent glutamate release and AMPA receptor activation[40] activates the BDNF-associated TrkB and mTORC1 pathway which promotes BDNF expression itself[51,52]. Of note, PSD-95, the postsynaptic marker that we found to be upregulated, controls activity-dependent AMPA receptor incorporation in the postsynapse[53,54] which can modify the strength of excitatory synaptic transmission[55].

Finally, an enrichment of differentially expressed genes associated with GO terms of learning, memory and cognition suggest behavioral long-term effects of the drug which are based on the above mentioned structural and functional modifications. The effects were dependent on the duration of drug exposure suggesting that repetitive administration of psilocybin might elicit beneficial effect with respect to brain plasticity.

Our study has some limitations. *The in vitro* system lacks metabolizing enzymes and the cellular complexity of brain tissue including glial cells. Furthermore, some experiments required prolonged psilocin exposure (96 hrs), which does not fully recapitulate the *in vivo* situation where psilocin is rapidly metabolized. Nevertheless, the majority of our key findings (BDNF upregulation, gene expression changes, neurite branching) were observed 24-48 hrs after a brief 10-minute exposure, more closely reflecting the post-acute effects observed *in vivo*.

Together, our work confirms the postulation by the Olson group that psychedelics may act through an evolutionary conserved mechanism as we can replicate the results from animal studies in our human system[25]. Our study underscores the significance of human-based models, particularly iPSC-derived cortical neurons, in elucidating the mechanisms of psychedelics and their potential for disease modeling and drug development. By leveraging these human-derived systems, the research emphasizes the translational potential of psychedelics, offering deeper insights into their action in a human context and advancing therapeutic innovation[56].

Supplementary Materials and Methods

Human material and generation of fibroblast-derived human iPSCs

The study was approved by the local ethics committee. All experiments with human material were in accordance with the Declaration of Helsinki. All healthy participants gave written informed consent. Reprogramming was done using CytoTune®-iPS 2.1 Sendai Reprogramming Kit (Thermo Fisher Scientific). Cells were cultured at 37°C, ambient O2 and 5% CO2 concentration under sterile conditions in an incubator (Binder). Applications with the cells were carried out in a sterile flow hood (Scanlaf Mars) by using sterile and autoclaved instruments and medium. Chromosomal alterations were excluded by genome-wide single nucleotide polymorphism (SNP) analysis and mycoplasma testing was performed on a regular basis. iPSCs were screened for their stem cell properties by the capability of *in vitro* differentiation into the three embryonic germ layers, ectoderm, mesoderm and endoderm and for pluripotent stem cells markers *in vitro*.

iPS cell culture

Fibroblast-derived iPS cells were kept as colonies under feeder free-conditions in stem cell state on 5% (v/v) Geltrex™-coated plates (Thermo Fisher Scientific) containing 1% (v/v) Pen/Strep (Thermo Fisher Scientific) in Essential 8 medium (DMEM/F12 with L-glutamine and HEPES (Thermo Fisher Scientific) supplemented with 1% (v/v) Pen/Strep (v/v), 64 µg/ml LAAP (Sigma-Aldrich), 14 ng/ml sodium selenite (Sigma-Aldrich), 200 ng/ml FGF-2 (154) (Cell Guidance Systems), 2 ng/ml TGF-β1 (Cell Guidance Systems), 20 µg/ml insulin (Sigma-Aldrich), 11 µg/ml transferrin (Sigma-Aldrich) that was changed daily. For passaging confluent iPS colonies were washed twice with phosphate buffered saline (DPBS) and then incubated with 0.5 mM EDTA (Thermo Fisher Scientific) for 5 - 10

min at RT until the colonies started to detach. After aspirating the EDTA solution the fractured colonies were gently resuspended in E8 medium containing 5 µM Rho-associated protein kinase (ROCK) inhibitor (Cell Guidance Systems).

Differentiation of iPS cells into neuronal progenitors

For *in vitro* differentiation into neural progenitors E8 medium was replaced by neural progenitor induction medium phase 1 (advanced DMEM/F-12 medium with glutamine (Thermo Fisher Scientific), with 1% (v/v) Pen/Strep (v/v), 2 mM GlutaMAX™ (Thermo Fisher Scientific), 1% (v/v) B-27 supplement with RA (Thermo Fisher Scientific), 10 µM SB-431542 (Cell Guidance Systems), 1 µM LDN-193189 (Stemcell Technologies), 2 µM XAV939 (Cell Guidance Systems) and 5 µM cyclopamine (Cayman Chemical) when iPS cells reached 70-80% confluency. At day 4, cells were dissociated 1:2 to a monolayer, continue using aforementioned medium. Upon day 8 cells were dissociated 1:2 and medium was changed to induction medium phase 2 (advanced DMEM/F-12 medium with glutamine with 1% (v/v) Pen/Strep, 2 mM GlutaMAX™, 1% (v/v) B-27 supplement with RA, 200 nM LDN-193189) for 8 more days. Finally, medium was changed to induction medium phase 3 (advanced DMEM/F-12 medium with glutamine with 1% (v/v) Pen/Strep, 2 mM GlutaMAX™, 1% (v/v) B-27 supplement with RA, 20 ng/ml FGF-2 (147) (Cell Guidance Systems). Dissociation into single cells was done using TrypLE™ (Thermo Fisher Scientific) for 5 - 15 min at 37 °C until the cells start to detach. Cells were then transferred with wash medium to a 15 ml tube and centrifuged for 4 min at 1000 g. The pellet was gently resuspended in corresponding neural progenitor induction medium supplemented with 5 µM ROCK inhibitor.

In vitro differentiation of neural progenitors into human cortical neurons

In vitro differentiation into human cortical neurons was launched by the change to neural differentiation medium phase 1, defined as day 0 of differentiation. Neural differentiation phase 1 medium consisted of neural base medium 1 (DMEM/F-12 medium with glutamine, 0.1% (v/v) GlutaMAX™, 1.8 mM $CaCl_2$ (Sigma-Aldrich), 1% (v/v) Pen/Strep, 1% (v/v) B-27, 0.5% (v/v) N2 supplement (prepared in the laboratory as follows: DMEM/F-12 with glutamine, 500 µg/ml insulin, 10 mg/ml transferrin, 520 ng/ml sodium selenite, 1.611 mg/ml putrescine (Sigma-Aldrich) and 630 ng/ml progesterone (Sigma-Aldrich)), 1% (v/v) NEAA (Thermo Fisher Scientific), 1.6 mg/ml glucose (Carl Roth)) supplemented with 200 µM ascorbic acid (Sigma-Aldrich), 1 µM LM22A (Sigma-Aldrich), 1 µM LM22B (Tocris Bioscience), 2 µM PD-0332991 (Selleckchem), 5 µM DAPT (Cell Guidance Systems) and was applied until day 3 of differentiation. The cells were split using TrypLE™ into phase 2 medium on polyethylenimine (Sigma Aldrich)/laminin (Sigma Aldrich) coated plates (1:2000 of 1% (PEI) in 25 mM boric acid (pH 8.4) (Thermo Fisher Scientific); 3.75 µg/ml laminin (Sigma Aldrich) in DPBS (Thermo Fisher Scientific). Neural differentiation medium phase 2 - 4 media consisted of neural base medium 2 with Neurobasal™ (Thermo Fisher Scientific) (plus 1.6 mg/ml glucose, 1% (v/v) Pen/Strep, 0.1% (v/v) GlutaMAX™ and 1% (v/v) B- 27) and was supplemented additionally to supplements of phase 1 medium with 3 µM CHIR99021 (Cell Guidance Systems), 10 µM forskolin (Cell Guidance Systems) and 300 µM GABA (Sigma-Aldrich). At day 10 of differentiation medium was changed to medium phase 3 containing, additionally to supplements of phase 1 medium, 3 µM CHIR99021. From day 17 on, CHIR99021 was removed in phase 4 and the medium contained 200 µM ascorbic acid, 1 µM LM22A, 1 µM LM22B and 2 µM PD-0332991. At day 24 medium was changed to neural differentiation phase 5 medium in neural base medium 3 (advanced MEM (Thermo Fisher Scientific), 1.6 mg/ml glucose, 1% (v/v) Pen/Strep, 0.1% (v/v) GlutaMAX, 1% (v/v) B-27) and 0.27 nM Bryostatin 1 (Merck Millipore) for the next 14 days. Medium was changed every 3-4 days half.

Co-culture of human cortical neurons with mouse astrocytes

For electrophysiological experiments mouse astrocytes were plated in a density of around 80,000 cells/well on PEI/laminin coated coverslips on 24-well plates. Mouse astrocytes were cultured in astrocyte standard medium, consisting of astrocyte base medium (1% (v/v) Pen/Strep, 0.5% (v/v)

N2, 1.6 mg/ml glucose) supplemented with 0.5% (v/v) N2, 1.6 mg/ml glucose, 0.1% B-27, 100 ng/µl epidermal growth factor (Cell Guidance Systems), 10 ng/ml FGF-2 (147) until they reached 80 - 90% density. Medium was changed every other day. 3 days before phase 1 neurons were split in a density of 200,000 cells onto the astrocytes the medium was changed to astrocyte differentiation medium, consisting of astrocyte base medium and 0.5% (v/v) N2, 1.6 mg/ml glucose and 10 ng/µl BMP-4 (Miltenyi Biotec). Medium was changed daily. Since the moment the cortical neurons were plated on the astrocytes the medium was changed to neural differentiation medium and differentiated was continued as described.

Neuroplasticity experiments in cortical neurons

For immunostainings around 200,000 cells/well (50,000 for Sholl analysis) were plated onto coverslips in 24-well plates. For WB, DNA- and RNA-based experiments around 2 - 6 million cells/well were plated on 6 well plate dishes or 10 cm dishes. Treatment of cortical neurons started at day 42 of differentiation. 3 days prior to experiments, for drug dissolving and during course of the experiment culture medium was replaced with neural base medium 3 containing 1% (v/v) Pen/Strep, 1.6 mg/ml glucose, 0,1% (v/v) GlutMAX™, 0,1% (v/v) B-27 and 200 µM ascorbic acid to avoid distorting effects of small molecules on cellular signal transduction pathways. For 7 days long-term treatment cells medium changes twice a week were performed with neural differentiation phase 5 medium.

Treatment of cortical neurons with psilocin

10 mM DMSO stock solution of light sensitive psilocin was diluted 1:1000 (final DMSO concentration = 0,001%) to a final concentration of 10 µM psilocin (THC-Pharm). For the short trigger mature cortical neurons were treated for 10 min with psilocin, washed once with advanced MEM containing 1% (v/v) Pen/Strep and were further cultured and then fixed or harvested after indicated time points post treatment. For the permanent treatment condition cells were treated for 24 (96) hrs permanently with 10 µM psilocin. For the 96 hrs plus 6 days washout condition cells were treated for 96 hrs permanently with 10 µM psilocin (fresh psilocin was replaced once), washed once and were further cultured in neural differentiation phase 5 medium.

Treatment of cortical neurons with ketanserin

To determine whether psilocin induced neuroplasticity effects were 5-HT2A-R dependent 75 mM DMSO stock solution of ketanserin (ApexBio) was diluted 1:1000 to a final concentration of 75 µM ketanserin (final DMSO concentration = 0,001%). Cells were pretreated with 75 µM ketanserin for 10 min to block the 5-HT2A-R, then treated for another 10 min with psilocin and ketanserin (final psilocin concentration = 10 µM, final ketanserin concentration = 75 μ M, final DMSO concentration = 0,002%), washed once with advanced MEM containing 1% (v/v) Pen/Strep and further cultured for 24 hrs post treatment.

Treatment of cortical neurons with dynasore

To determine whether psilocin induced neuroplasticity effects were endocytosis-mediated 100 mM DMSO stock solution of dynasore (Cayman Chemical) was diluted 1:2000 to a final concentration of 50 µM dynasore (final DMSO concentration = 0,0005%). Cells were pretreated with dynasore for 50 min to block endocytosis, then treated for another 10 min with psilocin (final psilocin concentration = 10 µM) and dynasore (final dynasore concentration = 50 µM; final DMSO concentration = 0,0015%), washed once with advanced MEM containing 1% (v/v) Pen/Strep and further cultured and then fixed after 24 h post treatment.

Immunocytochemistry

After a first washing with PBS, cells were fixed in 4% PFA (Sigma-Aldrich), washed three times with PBS and blocked and/or permeabilized in blocking solution containing 10% FBS (Thermo Fisher Scientific) in PBS. Blocking was performed for one h. Dilution of primary and secondary antibodies were performed in blocking solution. Please refer to Table S1 for blocking/

permeabilization solution and dilution of primary antibodies. Primary antibodies were incubated over night at 4°C. Samples were washed three times with corresponding blocking solution. Secondary antibodies, conjugated to Alexa Fluor 488, 568 or 647 (Thermo Fisher Scientific) were diluted 1:1000 and were applied for 1 h at room temperature (Table S2). Samples were then washed once in PBS to remove unbound antibodies. Counterstaining of cell nuclei was carried out by using 300 nM DAPI (Biolegend, Table S3), incubated for 5 min at room temperature and washed three times in PBS and once with ddH2O. Slides were mounted with mounting solution (100 mM Tris-HCl (pH 8.5), 25% glycerol, 10% mowiol (Carl Roth), 0.6% DABCO® (Carl Roth) on glass coverslip and air-dried overnight. Cells were observed with the Inverted Leica DMIL LED Microscope. Stem cell and neural progenitor properties were imaged with the Leica DM6 B microscope with Thunder imaging software. For neuroplasticity experiments Leica confocal TCS SP5 II microscope was used. Brightfield images were made with Fluorescence Microscope Celldiscoverer 7 microscope from Zeiss. For analysis of immunofluorescence a polygon selection of ROIs was chosen. The protein density and co-localization of particles was measured with the ComDet v.0.5.3 plug-in for ImageJ (National Institutes of Health (NIH), open source). A particle size (depending on experimenters' evaluation), constant for overall experiments (BDNF: 1.0; PSD-95: 3.0; Synapsin: 3.0) and an intensity threshold (in SD), adjusted within each experiment, was defined. For co-localization analysis the channels of proteins that have to be co-localized were merged in advance. As maximal distance between co-localized spots 4.00 pixels were stated. The number of particles was divided by the total length of the neurite in µm measured with the straight-line tool spanning the polygonal ROI. Multiple ROIs were set per image. N = 1 corresponds to one neurite segment detected by one ROI.

Antibody (clone)	Host species	Dilution	Blocking Solution in 10% Fetal bovine serum (FBS)	Manufacturer	Catalogue number	Registered office
BDNF	rabbit	1:300	0.1% Saponin	Elabscience	E-AB-18244.200	Houston, USA
CTIP-2 (25B6)	rat	1:500	0.3% Triton X	Abcam	ab18465	Cambridge, UK
cFOS (9F6)	rabbit	1:500	0.3% Triton X	Cell Signaling Technologies	2250	Danvers, USA
FOXA2	goat	1:500	0.3% Triton X	R&D Systems	AF2400	Minneapolis, USA
OCT3/4 (A-9)	mouse	1:500	0.3% Triton X	Santa Cruz	Sc-365509	Santa Cruz, USA
GFAP	mouse	1:500	0.1% Triton X	Synaptic Systems	173011	Göttingen, Germany
MAP2	chicken	1:7000	0.1% Saponin/ 0.1% - 0.3% Triton X	BioLegend	822501	San Diego, USA
mCherry	rabbit	1:1000	0.3% Triton X	Cell Signaling Technologies	43590S	Danvers, USA
NESTIN 196908	mouse	1:600	0.3% Triton X	R&D Systems	MAB-1259	Minneapolis, USA
NeuN (D4G4O)	rabbit	1:200	0.3% Triton X	Cell Signaling Technologies	24307S	Danvers, USA
PAX6 (Poly19013)	rabbit	1:500	0.3% Triton X	Biolegend	901301	San Diego, USA
PSD-95	rabbit	1:250	0.1% Saponin	Cell Signaling Technologies	2507S	Danvers, USA
SOX2 (D6D9)	rabbit	1:500	0.3% Triton X	Cell Signaling Technologies	3579S	Danvers, USA
Synapsin I/II/III (A17080A)	mouse	1:500	0.1% Saponin	BioLegend	853701	San Diego, USA
TAU	guinea-pig	1:700	0.1% Saponin/ 0.1% - 0.3% Triton X	Synaptic Systems	314004	Göttingen, Germany
TBR1	rabbit	1:500	0.3% Triton X	Abcam	ab31940	Cambridge, UK
vGLUT2	guinea-pig	1:200	0.1% Triton X	Synaptic Systems	135304	Göttingen, Germany

Table S1. Primary antibodies used for immunocytochemistry (ICC).

Antibody	Host species	Manufacturer	Catalogue number	Registered office
anti-chicken IgG Alexa Fluor-488	goat	Thermo Fisher Scientific	A11039	Waltham, USA
anti-guinea-pig IgG Alexa Fluor-488	goat	Thermo Fisher Scientific	A11073	Waltham, USA
anti-guinea-pig IgG Alexa Fluor-568	goat	Thermo Fisher Scientific	A11075	Waltham, USA
anti-mouse IgG Alexa Fluor-488	goat	Thermo Fisher Scientific	A11001	Waltham, USA
anti-mouse IgG Alexa Fluor-568	goat	Thermo Fisher Scientific	A11004	Waltham, USA
anti-rabbit IgG Alexa Fluor-488	goat	Thermo Fisher Scientific	A11008	Waltham, USA
anti-rabbit IgG Alexa Fluor-555	goat	Thermo Fisher Scientific	A21428	Waltham, USA
anti-rabbit IgG Alexa Fluor-647	goat	Thermo Fisher Scientific	A21244	Waltham, USA
anti-rat IgG Alexa Fluor-555	goat	Thermo Fisher Scientific	A21434	Waltham, USA

Table S2. **Secondary antibodies used for ICC.**

Antibody (clone)	Dilution	Manufacturer	Catalogue number	Registered office
4,6-diamidino-2-phenylindole (DAPI)	300 nM	Biolegend	422801	San Diego, USA

Table S3. **Fluorescent probes.**

Analysis of neuronal complexity

For Sholl analysis around 50,000 cells/well were cultured on 24 well PEI/laminin coated coverslips. Cells were transduced 2 weeks before psilocin treatment with adeno-associated virus AAV_CamKIIa p- hCHR2(134a)-mCherry (friendly provided by AG Grinevich, Central Institute of Mental Health, Mannheim, Germany), when mCherry expression was visible by microscope. Cells were fixed after indicated treatment timepoints. Images were analyzed using the Sholl analysis plug-in of ImageJ (circle radii). Start radius: 25 µm, step size: 25 µm, end radius: 125 µm, set center from active ROI, preview). Crossings were calculated manually. Based on that, total length and sum of intersections were calculated. N = 1 corresponds to one neuron.

Protein isolation and measurement of protein concentration

Cells (1 well of 6 well plate) were washed with ice cold DPBS, harvested by using a cell lifter and were transferred into a 1.5 ml tube on ice. In the following the cells were centrifuged for 5 min at 5000 g at 4 °C. The supernatant was removed and the sample was stored at - 20°C. For protein isolation, cells were resuspended in 150 µl of protein lysis buffer (50 mM Tris-HCL (pH 7.4), 150 mM NaCI, 25 mM EDTA, 1% (v/v) SDS with one protease and one phosphatase inhibitor mini tablet (Thermo Fisher Scientific) per 10 ml of protein solution) and incubated for 10 min at room temperature and then incubated 1 h on ice. To shear gDNA and reduce viscosity samples were sonicated (20% duty cycles, 50% output, five pulses) from a Branson Ultrasonics™ sonifier 250 (Thermo Fisher Scientific). Samples were centrifuged for 5 min for 5000 g at 4°C. Supernatant was transferred to a new tube. Protein concentration was measured with the BCA protein assay (Thermo Fisher Scientific) following the manufacturer's instructions. Samples were diluted 1:5 in

ddH$_2$O and the absorption at 562 nm was measured in a PowerWave™ XS microplate reader (BioTek). The protein concentration of samples was calculated based on the included BSA standard dilution series.

SDS-polyacrylamide gel electrophoresis and western immunoblotting

15 - 30 µg of protein was mixed with 6x denaturing protein sample buffer (93.75 mM Tris-HCL (pH 6.8), 6% SDS, 6% Glycerol, 9% 2-Mercaptoethanol, 0.25% Bromophenol blue) and boiled for 5 min at 95 °C. For the separation of proteins an SDS-PAGE (Bio-Rad Laboratories) was performed in a Mini- PROTEAN 2-D electrophoresis cell chamber and with the PowerPac™ Basic Power Supply. First, the polyacrylamide gel (Gel buffer for polyacrylamide gels, SDS-PAGE: 3M Tris-HCl (pH 8.5), 0.3% (w/v) SDS; SDS-Polyacrylamide, stacking gel: 24.8% (v/v) Gel buffer, SDS-PAGE, 3.84% (v/v) Bis/ acrylamide, 0.00672% (w/v) APS, 0.224% TEMED; SDS-Polyacrylamide, separating gel: 33.3% (v/v) Gel buffer, SDS-PAGE, 10% (v/v) Bis/ acrylamide, 10% (v/v) glycerol, 0.028% (w/v) APS, 0.09% (v/v) TEMED) runs for about 30 min with 30 V for stacking of proteins and then for about 1.5 - 2 hrs at 110 V. A semi-dry blotting was performed using the Trans-Blot Turbo™ transfer system (Bio-Rad Laboratories) performed with 20 V and 1 A for 30 - 60 min. A reference protein marker (PS10 plus, GeneON Bioscience) was included to determine the size of the protein bands. For blotting 0.45 µm pore size nitrocellulose blotting membrane (Sigma-Aldrich) was used. The membrane was surrounded from both sides by 6 layers of WB filter tissue (VWR). Filter tissue and membrane were wetted in transfer buffer (10% (v/v) Tris-glycine buffer, 20% (v/v) methanol, 0.08% (v/v) SDS). Membranes were blocked for 60 min in 5% BSA (Sigma-Aldrich) in TBS-T (10% (v/v) of TBS with 248 mM Tris-HCl (pH 7.4), 1.37 M NaCI, 26.8 mM KCl plus 0.1% (v/v) Tween®20 (Sigma-Aldrich)) in a 50 ml tube. Primary antibodies (Table S4) were diluted in 5% BSA in TBS-T and were incubated over night at 4°C or for 1 h at room temperature on a rolling mixer. The membrane was washed three times in TBS-T for 10 min at room temperature on the next day. 1:15,000 infrared DyLight™ IR-conjugated secondary antibodies (Cell Signaling Technologies, Table S5) in TBS-T were applied for 1 h at room temperature. Washing in TBS- T was carried out three times and once in TBS for 10 min at room temperature. Visualisation of tagged proteins was carried out with Odyssey IR WB imaging system (Li-COR). Signals were normalized by 1: 20,000 p-actin levels. Antibodies for Western blotting are listed in Supplementary Table S4. For quantification region of interests (ROIs) were set around lanes and intensity was measured with the densitometry analysis in ImageJ.

Antibody (clone)	Host species	Dilution	Manufacturer	Catalogue number	Registered office
Actin (8H10D10)	mouse	1:20,000	Cell Signaling Technologies	3700S	Danvers, USA
Actin (13E5)	rabbit	1:20,000	Cell Signaling Technologies	4970S	Danvers, USA
AKT (pan) (C67E7)	rabbit	1:2500	Cell Signaling Technologies	4691S	Danvers, USA
BDNF	rabbit	1:500	Elabscience	18244.200	Houston, USA
pAKT (S473) D9E XP®	rabbit	1:2500	Cell Signaling Technologies	4060S	Danvers, USA
pTrkB	mouse	1:500	Santa Cruz	SC-8058	Santa Cruz, USA

Table S4. Primary antibodies used for Western blotting (WB).

Antibody (clone)	Host species	Manufacturer	Catalogue number	Registered office
Anti-mouse DyLight™ 680	goat	Cell Signaling Technologies	5470S	Danvers, USA
Anti-mouse DyLight™ 800	goat	Cell Signaling Technologies	5257S	Danvers, USA
Anti-rabbit DyLight™ 680	goat	Cell Signaling Technologies	5366S	Danvers, USA
Anti-rabbit DyLight™ 800	goat	Cell Signaling Technologies	5151S	Danvers, USA

Table S5. IR-dye conjugated secondary antibodies used for WB. Secondary antibodies were diluted 1:15,000.

Ribonucleic acid isolation

For Ribonucleic acid (RNA) isolation cells were (2 wells of 6well plate) resuspended in 500 µl peqGold Trifast™ (VWR) and incubated for 10 min at room temperature. 100 µl of chloroform (Sigma-Aldrich) was added to the lysate and incubated for 10 min at room temperature. Tubes were then centrifuged for 5 min at 12,000 g at 4°C. The upper clear, aqueous nucleic acid phase was transferred into a new tube. 250 µl of isopropanol (Th. Geyer) was added to each sample. For RNA precipitation tubes were kept overnight at - 20°C. Then, tubes were centrifuged for 15 min at 4°C of 12,000 g and supernatant was discarded. The pellet was washed twice with 75% ethanol (Th. Geyer) in DEPC water (Carl Roth) and centrifuged for 10 min at 4 °C at 12,000 g. After the last washing step all ethanol had to evaporate by first discarding the ethanol and afterwards letting air-dry the pellet for about 30 min. The pellet was resuspended in 20 µl DEPC-treated H2O and shook at 400 rpm at 37 °C. To prevent DNA contamination the DNAase I Amplification grade kit (Sigma-Aldrich) was used.

Synthesis of complementary DNA

Complementary DNA (cDNA) was synthesized via the iScript™ cDNA synthesis kit (Bio-Rad Laboratories) according to manufacturer's instructions. 500 ng - 1 pg cDNA was used to reversely transcribe RNA into cDNA. Standard cycling program for cDNA synthesis: 25 °C for 5 min, 46 °C for 20 min, 95°C for 1 min. The resulting cDNA was diluted 1:5 in nuclease-free H2O. (1x) Taq reaction buffer (Biozym), each 200 µM 10 mM dNTP mix (Steinbrenner Laborsysteme), each 400 nM 10 µM primer mix, 0.625 U Taq DNA polymerase (5 U/pl) (Biozym), 0.4 - 10 ng Template DNA). Standard RT-PCR cycling program: Samples were denatured by heating at 95 °C for 1 min followed by 35 cycles of amplification and quantification (95°C for 15 s and 60 °C for 15 s and 72°C for 10 s) and by a final extension cycle (72 °C, 5 min). Primers for real-time (RT)- polymerase chain reaction (PCR) are listed in Supplementary Table S6.

Primer name	Sequence (5'->3')	Size base pair (bp)
HTR2A-For	TTGGGCTACAGGACGATT	383
HTR2A-Rev	GAAGAAAGGGCACCACATC	
18s rRNA-For	AAACGGCTACCACATCCAAG	143
18s rRNA-Rev	CCTCCAATGGATCCTCGTTA	
ANK3-For	TGGAATGATTGAACGGAGTACAGG	142

ANK3-Rev	AGTGAAGCCTGACTTGGCTG	
ARC-For	TCAGCTCCAGTGATTCACGC	163
ARC-Rev	GGGAACCTTGAGACCTGTTGT	
BDNF-For	TTTGGTTGCATGAAGGCTGC	199
BDNF-Rev	TGAGGACCAGAAAGTTCGGC	
BCL11B-For	CAACCCGCAGCACTTGTC	80
BCL11B-Rev	CCTCGTCTTCTTCGAGGATGG	
DLG4-For	AGCCCCAGGATATGAGTTGC	90
DLG4-Rev	CCCAGACCTGAGTTACCCCT	
FOS-For	CAAGCGGAGACAGACCAACT	177
FOS-Rev	AGTCAGATCAAGGGAAGCCA	
GAD1-For	ATCCTGGTTGACTGCAGAGAC	80
GAD1-Rev	CCAGTGGAGAGCTGGTTGAA	
GRIA2-For	GGATCCTCATTAAGAACCCCAGT	148
GRIA2-Rev	TGAGGGCACTGGTCTTTTCC	
GRIA4-For	AGGTGAATGTGGACCCAAGG	177
GRIA4-Rev	AAGGTCAGCTTCATTCTCTTCG	
GRIN1-For	GGCAACACCAACATCTGGAA	71
GRIN1-Rev	CCATCCGCATACTTGGAAGAC	
GRIN2B-For	CTCACCCCCTTTCCGCTTT	156
GRIN2B-Rev	AAGGCATCCAGTTTCCCTGTT	
NEUROD6-For	ACTCAGCCTGAAAAGATTTGG	89
NEUROD6-Rev	TGGTTCTCTAATCTTAAATTACCTT	
NPAS4-For	AACACTACCGCCTGTTGGC	133
NPAS4-Rev	GCAGTAATGGGTCCCTCTGG	
NRXN1-For	GTGTTTTGCCGGTGCTGTTA	133
NRXN1-Rev	CTTTTACCTTGGTCGCCCATC	
RBFOX3-For	GCGCTGAGCCCGTTGAAAT	104
RBFOX3-Rev	CTCCTTCTGGACCGTCCTTG	
Mycoplasma-For	GGGAGCAAACAGGATTAGATACCCT	> 200

Mycoplasma-Rev	TGCACCATCTGTCACTCTGTTAACCTC	
SLC17A7-For	AGCTGGGATCCAGAGACTGT	116
SLC17A7-Rev	CCGAAAACTCTGTTGGCTGC	
SLC17A6-For	TCAGATTCCGGGAGGCTACA	175
SLC17A6-Rev	TGGGTAGGTCACACCCTCAA	
SV2A-For	AACCTAGACCAGGCACTCAT	99
SV2A-Rev	ACCCCTCCCCACAGTTACTTA	
SYN1-For	CAGCTCAACAAATCCCAGTCTC	99
SYN-1Rev	GGTCTCAGCTTTCACCTCGT	
TBR1-For	ACGAACAACAAAGGAGCTTCA	68
TBR1-Rev	TGGTACTTGTGCAAGGACTGTA	
TUBB3-For	GAGCGGATCAGCGTCTACTA	77
TUBB3-Rev	GGTTCCAGGTCCACCAGAA	

Table S6. Primers for RT-PCR.

For expression control total human adult (BioCat) and fetal brain (Tebu Bio) was included.

Agarose gel electrophoresis

Samples were mixed with 10 x DNA sample buffer (50 mM Tris-HCl, pH 7.6, 0.25% (w/v) Bromphenol blue, 60% Glycerol). DNA fragments were separated in a 1 - 2% (w/v) agarose gel in 1x TAE buffer (40 mM Tris, 20 mM acetic acid, 1 mM EDTA), containing 1: 15,000 peqGreen (VWR) for staining of DNA. A reference DNA marker (100 bp or 1 kbp, New England Biolabs) was included to determine the size of the amplicons. Gels run for 50 min at 100 V and were imaged on a GeneFlash imaging system (Syngene).

RNA Bulk Sequencing and Analysis

For each sample, 30 µl of RNA solution (60 ng/µl) in ddH2O was sent to the High Throughput Sequencing (seq) Unit of the Genomics & Proteomics Core Facility at the DKFZ (Heidelberg, Germany) to be processed for RNA Bulk Sequencing. Samples were run through in-house quality control and only samples with an RNA integrity number (RIN) ≥ 5.0 were used for cDNA library preparation according to the TruSeq Stranded protocol (Illumina). Libraries were sequenced to 50 bp paired reads on the Illumina NovaSeq 6K platform to an average of 40 M reads per sample. The DKFZ Omics IT and Data Management Core Facility performed the RNAseq processing workflow. Total counts per feature were imported to R[59] (v. 4.0.3-4.2.2) and analysed using DESeq2[60] (v. 1.30.1-1.38.3). All features without any counts were removed, for differential testing with DESeq2 the formula "|Batch+Cell_line+Condition_simple" was used. Differentially expressed genes (padj <=.05) were used to perform gene ontology (GO) enrichment analysis and Kyoto Encyclopedia of Genes and Genomes (KEGG) enrichment analysis with the clusterProfiler v 4.8.3 package[61]. The organism database used for this analysis was org.Hs.eg.db[62] (v. 3.17.0). GO Chord Plots were created using GOplot (v. 1.0.2)[63].

Zscores in GO plots showing up/downregulated genes were calculated with the following formula: zscore=(up-down)/sqrt(count). Heatmaps for RNAseq expression data show z-scaled DESeq2 normalized counts. Biological batch replicates of each samples ensured intra-cell lines stability of

results. The R code used to analyze RNAseq data is available at *https://github.com/ahoffrichter/Schmidt* et al 2025.

Electrophysiology

Whole-cell patch-clamp recordings from iPSC-derived cortical neurons on PEI/laminin-coated coverslips cultured on mouse astrocyte cells were made using an EPC9 amplifier and PatchMaster (HEKA Elektronik GmbH). The neurons were identified with a Zeiss Axioskop using infrared differential interference contrast video microscopy in the recording chamber. Neurons were perfused at 2 ml/min (peristaltic pump; Ismatec GmbH) with carbogen (95% O2; 5% CO2)-saturated artificial cerebrospinal fluid (ACSF) containing 125 mM NaCl, 1 mM $MgCl_2$, 2 mM $CaCl_2$, 2.5 mM KCl, 10 mM D-glucose, 25 mM $NaHCO_3$, 1.25 mM NaH_2PO_4 (pH 7.3, osmolarity 300 mOsm). Pipettes were pulled from borosilicate glass capillaries (GB150F-8P, 1.5 mm o.d., 0.86 i.d.; Science Products GmbH) with a P-97 micropipette puller (Sutter Instrument). Pipettes had resistances between 4-6 MQ when filled with intracellular solution containing 115 mM K-gluconate (or cesium-gluconate), 20 mM KCl, 10 mM Na- phosphocreatine, 4 mM Mg-ATP, 0.3 mM GTP, 0.2 mM ethylene glycol tetraacetic acid (EGTA) and 10 mM HEPES (pH 7.3, osmolarity 300 mOsm). In voltage-clamp, input resistance was determined at -70 mV based on currents evoked by small voltage steps (-3 mV; 300 ms). In current-clamp, the resting membrane potential (RMP) was determined and APs were evoked with increasing current injections (10 pA; 300 ms). The amplitude of the first evoked AP was analyzed, and the number of all APs evoked by 10 depolarizing steps was summed up. sEPSCs were recorded at -70 mV with K (Fig. 5B)- or Cs (Fig. 5D and Fig. S4B) -based intracellular solution. Miniature EPSCs (mEPSCs) were recorded at -70 mV in 1 µM TTX and with Cs-based intracellular solution. Recordings were made at room temperature and were sampled at 20 kHz. Offline analysis was done with FitMaster (HEKA Elektronik GmbH). Spontaneous synaptic activity was analyzed using MiniAnalysis (Synaptosoft).

Statistical analysis visualization

Unless indicated otherwise, data for quantitative analysis was based on at least two genetically independent cell lines with two independent biological replicates. For statistical analysis the RStudio for macOS (Version 1.4.1106© 2009) was used. Graphs were generated with RStudio and show mean including single data points ± standard error of mean (SEM) or violin blots including single data points (scatterplot) with mean ± standard deviation (SD) and boxplot with median. The Kolmogorov-Smirnov test for equality of a probability distribution and the Levene test for homogeneity of variance were calculated prior statistical analysis. In case the data does not meet the assumption for parametric testing Kruskal-Wallis test for more than two group comparisons (post hoc Wilcoxon rank sum test, p-value adjustment Bonferroni correction), or for a two group comparison a Mann-Whitney-U-test for independent samples was calculated. Significance levels against the respective controls were not significant (n.s) if $p > .05$, or significant *$p < .05$. Individual figure legends contain detailed information regarding the number of replicates, sample size and the applied statistical tests. Graphic illustrations were generated with *Biorender.com* (BioRender).

Supplementary figures

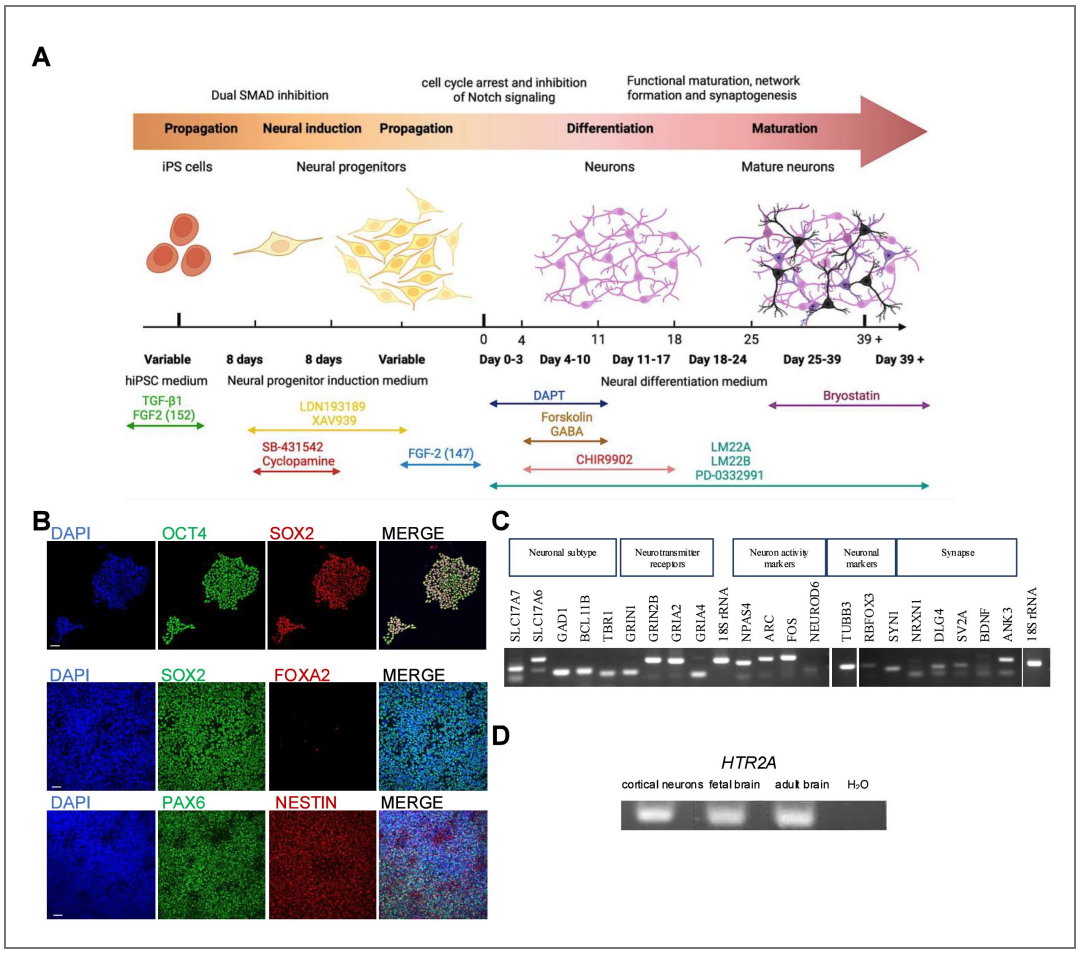

Suppl. Fig. 1. Validation of iPSC and neural progenitor properties and *HTR2A* gene expression. (A). Timeline: hiPSCs were differentiated *in vitro* into glutamatergic cortical neurons over a neuronal progenitor step. Maturation of cortical neurons took about 6 weeks. Scheme created in BioRender, Ladewig, J. (2025) *https://BioRender.com/v84c084* (B) iPSCs expressed pluripotent marker SOX2 and OCT4. Neuronal progenitors expressed SOX2, PAX6 and NESTIN and were negative for FOXA2 as a midbrain marker. Scale bar: 50 pm. (C) RT-PCR analysis revealed expression of neuronal subtype markers, neurotransmitter receptors, neuronal activity markers, neuronal markers and synapse- associated genes. (D) RT-PCR of the *HTR2A* gene (also expressed in commercialized samples of fetal and adult brain) confirmed expression of 5-HT2A-R. Scale bar: 50 pm.

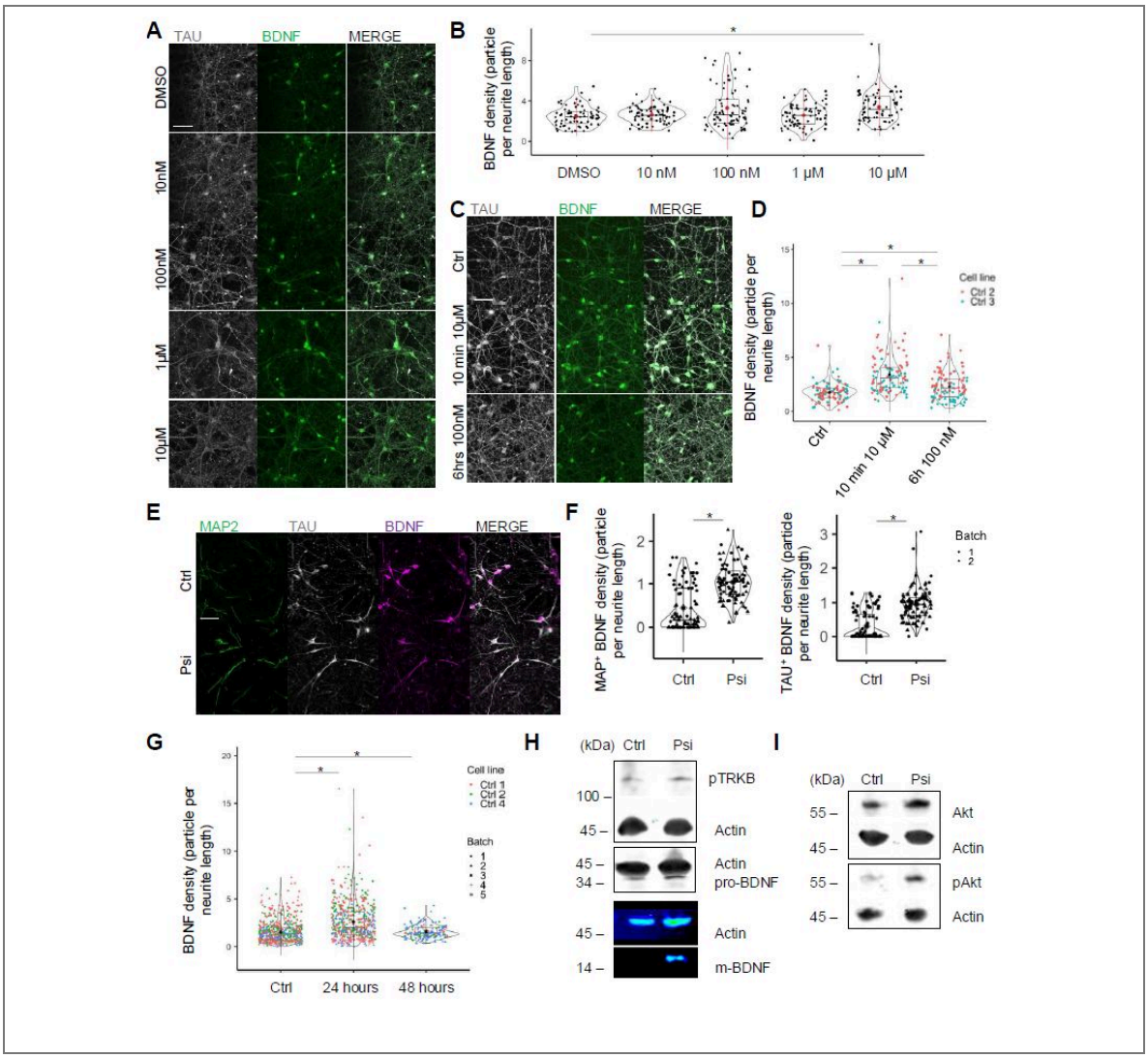

Suppl. Fig. 2. Influence of different treatment conditions on BDNF level.

(A) Representative image of a neuronal network for pre-treatment condition (DMSO) and 24 hrs after a 10 min 10 nM, 100 nM, 1 µM or 10 µM trigger showed the strongest increase in BDNF density for the 10 µM treatment condition. Scale bar: 50 pm. (B) BDNF density was exclusively significantly increased 24 hrs after 10 min 10 µM Psilocin trigger (10 pM). Ctrl cell line 1 was included in the analysis, with one biological batch (Ctrl with N = 76 neurites; 24 hrs after a 10 min 10 nM (N = 75 neurites), respectively 100 nM (N = 75 neurites), respectively 1 µM (N = 75 neurites), respectively 10 µM (N = 75 neurites). (C) Representative image of a neuronal network 24 hrs after an "artificial" (10 min 10 pM) and a "physiological" (6 hrs 100nM) treatment condition. Scale bar: 50 pm. (D) BDNF density was significantly increased 24 hrs after a 10 min 10 µM psilocin trigger (10 min 10 pM) and 24 hrs after a 6 hrs 100 nM psilocin stimulation (6 hrs 100 nM). BDNF density was also significantly increased for the" artificial" compared to the "physiological" stimulation. Two Ctrl cell lines were included in the analysis, each with one biological batch (Ctrl with N = 99 neurites; 10 min 10 µM with N = 102 neurites; 6 hrs 100 nM with N = 102 neurites). (E) Representative image of a neuronal network of the Ctrl condition and 24 hrs after a 10 min 10 µM psilocin trigger showed an increase in axonal TAU+ and dendritic MAP2+ BDNF density. Scale bar: 50 pm. (F) BDNF density was significantly increased for axonal TAU+ and dendritic MAP2+ BDNF density for the psilocin condition. One cell line (Ctrl 3) was included in the analysis, with two biological batches (Ctrl with N = 90 neurites; Psi with N = 90 neurites). (G) BDNF density was significantly increased 24 and still 48 hrs (24 hrs; 48 hrs) after a 10 min 10 µM psilocin trigger. Three Ctrl cell lines were included in the analysis (Ctrl with N = 520 neurites; 24 hrs with N = 478 neurites; 48 hrs with N = 170 neurites). (H) Endogenous phosphorylated (activated) TrKB (pTrkB) receptor, pro- BDNF and m-BDNF protein level increased 24 hrs after psilocin (Psi) administration. (I) Representative WB: phosphorylated AKT (pAKT) protein level, indicating an activation of pro survival AKT pathway, was increased 24 hrs after psilocin (Psi) exposure. For all analyses Kruskal-Wallis-Test for independent samples was calculated. Post hoc Wilcoxon rank sum test. Bonferroni-correction, adjusted $p < .05$, mean ± SD. Significance levels against the respective control are *$p < .05$.

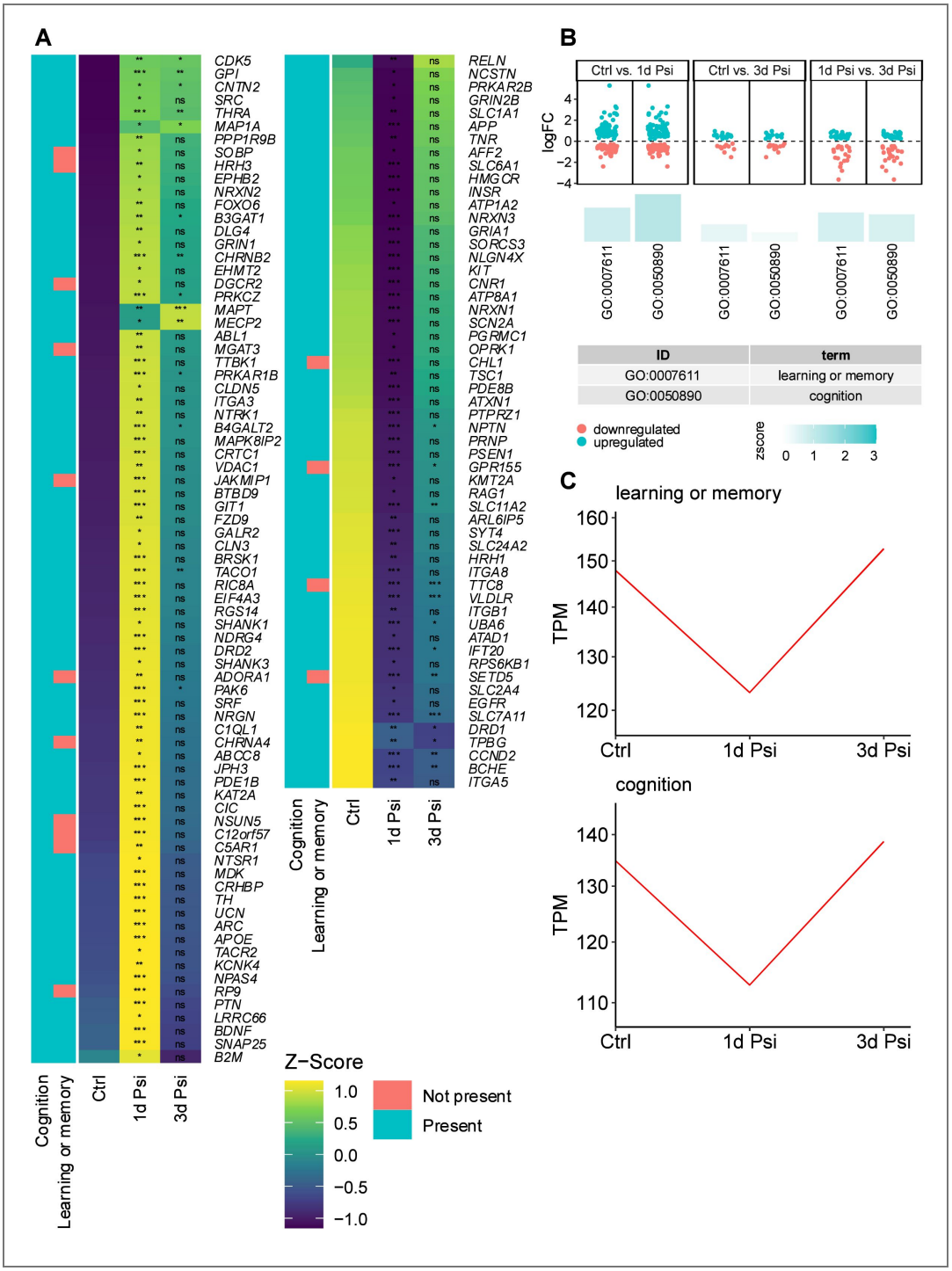

Suppl. Fig. 3. Psilocin displays fast and enduring changes on GO terms related to learning, memory and cognition.

(A) Heat map (z-scaled normalized counts) showing expression of genes that are grouped in the selected GO term related to "cognition". Genes that are also present in the GO term related to "learning and memory" are stated as "present", indicating great overlay of the genes of the two GO terms. (B-C) Psilocin induced within 24 hours a first "shaking" wave of selected GO genes based on DESeq2 normalized counts. After 3 days those GO genes normalized. (B) Log2fold changes of each gene between two conditions are shown as dots. Zscores indicate if more genes in the respective GO term are upregulated or downregulated indicated by height and color of the bars. (C) TPM-normalized mean (red line) of psilocin-induced temporal expression pattern of genes belonging to the indicated GO. Shaded area is indicating SD. TPM, transcripts per kilobase million. Significance levels against the respective control ns: p-adj. > .05, *: p-adj. <= .05, **: p-adj. <= .01, ***: p-adj. <= .001.

Suppl. Fig. 4. **Psilocin-induced increase in synaptic strength.**

(A) Increase in mEPSCs amplitude at day 7 after 24hrs permanent psilocin administration. Ctrl 2 with N = 16 cells, Psi 24hrs; day 7 with N = 14 cells. (B) Significant increase in sEPSCs amplitude 6 days after 96 hrs permanent 10 µM psilocin administration (Psi 96hrs; day 10). Ctrl 2 with N = 8 cells, Psi 96hrs; day 10 with N = 9 cells. For all experiments Mann-Whitney-U-test for independent samples was calculated, mean ± SEM. Significance levels against the respective control are *p < .05.

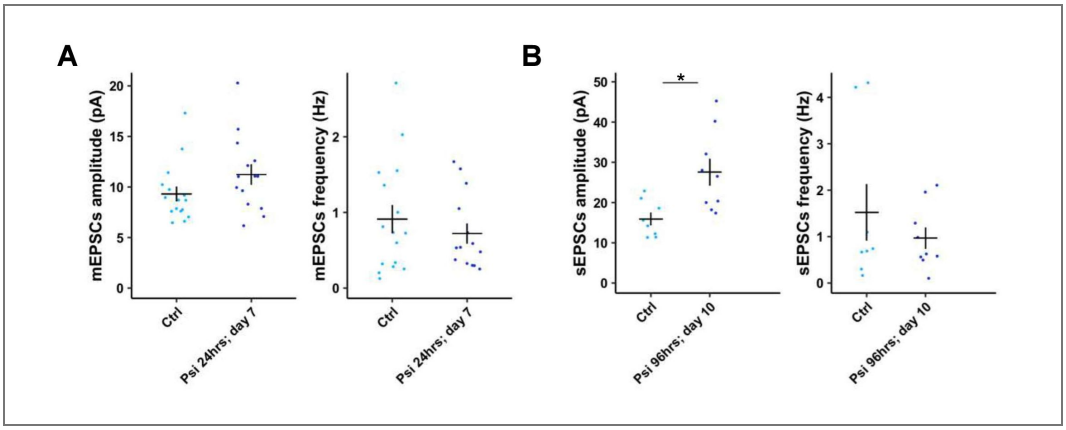

Suppl. Fig. 5. **Simplified schematic of signal transduction pathways proposed to mediate psychedelic-induced neuroplasticity in the cortex.**

Serotonergic psychedelics activate the 5-HT2A receptor (5-HT2A-R), triggering G-protein-coupled PLC and PLA2 pathways, which, similar to m-BDNF-TrkB activation, increase intracellular Ca^{2+} and PKC activity. BDNF-TrkB signaling further activates mTOR and NMDAR-dependent plasticity via the PI3K/AKT pathway. Psychedelic-induced glutamate release promotes mTOR activation and BDNF release through AMPARs, enhancing glutamatergic signaling and IEG (e.g., c-FOS) expression. 5- HT2A-R also interacts with PSD-95, while PI3K, ERK1/2, and CaMK activate CREB, stimulating *BDNF* transcription. Image created using *BioRender.com*, adapted from[24] and used in[57]. Abbreviations: 5-HT, serotonin; AKT, protein kinase B; AMPAR, a-amino-3-hydroxy-5-methyl-4- isoxazolepropionic acid receptor; BDNF, brain-derived neurotrophic factor; CaMK, Ca^{2+}/calmodulin-dependent kinase; CREB, cAMP response element-binding protein; ERK1/2, extracellular signal- regulated kinase 1/2; IEG, immediate early gene; MAPK, mitogen-activated protein kinase; mTOR, mammalian target of rapamycin; NMDAR, N-methyl-D-aspartate receptor; PI3K, phosphoinositide 3- kinase; PKC, protein kinase C; PLA2, phospholipase A2; PLC, phospholipase C; PSD-95, postsynaptic density protein 95; TrkB, tropomyosin receptor kinase B.

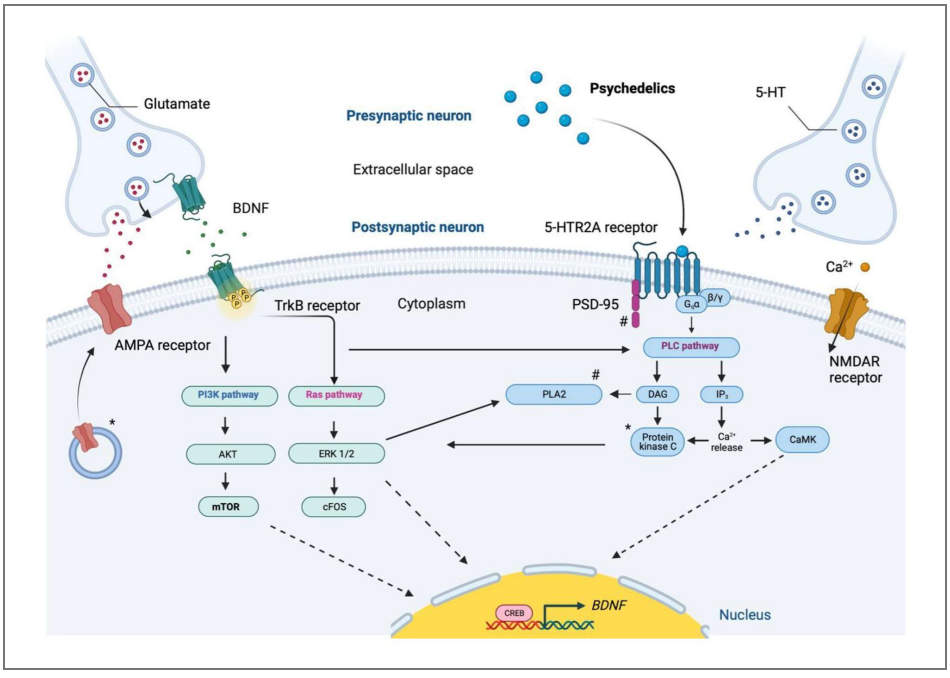

Data availability

The primary data supporting the findings of this study are available from the authors upon reasonable request. The R code used to analyze RNAseq data is available at *https://github.com/ahoffrichter/Schmidt_et_al_2025*.

Acknowledgements

We thank Isabell Moskal, Gina Tillmann and Helene Schamber for the excellent technical support. This work was supported by the Bundesministerium für Bildung und Forschung (BMBF, SysmedSUD, Grant 01EK2101B), and the Hector Stiftung II. We thank Valery Grinevich (Department of Neuropeptide Research) for providing the AAV. This work was previously published as an abstract and poster at the following conferences: ISSCR 2021, eMed 2021 + 2022, GSCN 2022 + 2025, ICPR 2024.

Additional information

Author contributions

MS designed the study, performed the experiments, analyzed the data and wrote the manuscript. AH conducted processing, analysis and visualization of bulk RNA sequencing data. MD and GK performed electrophysiological characterization of neuronal cultures supplied by MS. SH generated the iPS cell lines Ctrl 1, Ctrl 2, Ctrl 3, Ctrl 4. JL, GK and TL edited the manuscript. TL was scientific consultant. MM and RS provided psilocin and edited the manuscript. PK conceptualized the study, supervised the work, provided resources and edited the manuscript.

Author ORCID iDs

Anne Hoffrichter: https://orcid.org/0000-0001-6009-7826
Marcus W Meinhardt: https://orcid.org/0000-0002-5103-0731
Julia Ladewig: https://orcid.org/0000-0002-5943-7990
Philipp Koch: https://orcid.org/0000-0003-3713-8786

Author notes

Conflict of Interest Authors M.S. and P.K. are listed as inventors on a filed patent application related to the treatment of neurological diseases by modulating brain BDNF. All other authors declare no competing interest.
Corresponding author: Prof. Dr. Philipp Koch, Hector Institute for Translational Brain Research, Central Institute of Mental Health, Square J5, 68159 Mannheim, Germany. Phone: +49 621 1703 6711

References

1. **Nichols D,** Johnson M, Nichols C (2017) Psychedelics as Medicines: An Emerging New Paradigm. *Clin Pharmacol Ther* **101**:209-219 https://doi.org/10.1002/cpt.557
2. **Carhart-Harris RL,** Goodwin GM (2017) The Therapeutic Potential of Psychedelic Drugs: Past, Present, and Future. *Neuropsychopharmacology* **42**:2105-2113 https://doi.org/10.1038/npp.2017.84
3. **Miller G** (2010) Is pharma running out of brainy ideas?. *Science* **329**:502-504 https://doi.org/10.1126/science.329.5991.502
4. **Schenberg EE** (2018) Psychedelic-Assisted Psychotherapy: A Paradigm Shift in Psychiatric Research and Development. *Front Pharmacol* 9 https://doi.org/10.3389/fphar.2018.00733
5. **Vargas M V.,** Meyer R, Avanes AA, Rus M, Olson DE (2021) Psychedelics and Other Psychoplastogens for Treating Mental Illness. *Front Psychiatry* 12 https://doi.org/10.3389/fpsyt.2021.727117

6. **Carhart-Harris RL,** Bolstridge M, Day CMJ, et al. (2018) Psilocybin with psychological support for treatment-resistant depression: six-month follow-up. *Psychopharmacology (Berl)* **235** https://doi.org/10.1007/s00213-017-4771-x
7. **Grob CS,** Danforth AL, Chopra GS, et al. (2011) Pilot study of psilocybin treatment for anxiety in patients with advanced-stage cancer. *Arch Gen Psychiatry* **68**:71-78 https://doi.org/10.1001/archgenpsychiatry.2010.116
8. **Ross S,** Bossis A, Guss J, et al. (2016) Rapid and sustained symptom reduction following psilocybin treatment for anxiety and depression in patients with life-threatening cancer: a randomized controlled trial. *J Psychopharmacol* **30** https://doi.org/10.1177/0269881116675512
9. **Moreno FA,** Wiegand CB, Taitano EK, Delgado PL (2006) Safety, Tolerability, and Efficacy of Psilocybin in 9 Patients With Obsessive-Compulsive Disorder. *J Clin Psychiatry* **67**:1735-1740 https://doi.org/10.4088/JCP.v67n1110
10. **Bogenschutz MP,** Ross S, Bhatt S, et al. Percentage of Heavy Drinking Days Following Psilocybin-Assisted Psychotherapy vs Placebo in the Treatment of Adult Patients With Alcohol Use Disorder. JAMA Psychiatry. Accessed Published online August 24, 2022 https://doi.org/10.1001/jamapsychiatry.2022.2096
11. **Johnson MW,** Garcia-Romeu A, Griffiths RR (2017) Long-term follow-up of psilocybin-facilitated smoking cessation. *Am J Drug Alcohol Abuse* **43** https://doi.org/10.3109/00952990.2016.1170135
12. **Holze F,** Vizeli P, Ley L, et al. (2021) Acute dose-dependent effects of lysergic acid diethylamide in a double-blind placebo-controlled study in healthy subjects. *Neuropsychopharmacology* **46**:537-544 https://doi.org/10.1038/s41386-020-00883-6
13. **Nichols DE** (2016) Psychedelics. *Pharmacol Rev* **68**:264-355 https://doi.org/10.1124/pr.115.011478
14. **Rickli A,** Moning OD, Hoener MC, Liechti ME (2016) Receptor interaction profiles of novel psychoactive tryptamines compared with classic hallucinogens. *Eur Neuropsychopharmacol* **26** https://doi.org/10.1016/j.euroneuro.2016.05.001
15. **Glennon RA,** Titeler M, McKenney JD (1984) Evidence for 5-HT2 involvement in the mechanism of action of hallucinogenic agents. *Life Sci* **35**:2505-2511 https://doi.org/10.1016/0024-3205(84)90436-3
16. **Vollenweider FX,** Vollenweider-Scherpenhuyzen MF, Babler A, Vogel H, Hell D (1998) Psilocybin induces schizophrenia-like psychosis in humans via a serotonin-2 agonist action. *Neuroreport* **9** https://doi.org/10.1097/00001756-199812010-00024
17. **Gonzalez-Maeso J,** Weisstaub N v, Zhou M, et al. (2007) Hallucinogens recruit specific cortical 5-HT(2A) receptor-mediated signaling pathways to affect behavior. *Neuron* **53** https://doi.org/10.1016/j.neuron.2007.01.008
18. **Kometer M,** Schmidt A, Jancke L, Vollenweider FX (2013) Activation of Serotonin 2A Receptors Underlies the Psilocybin-Induced Effects on Oscillations, N170 Visual-Evoked Potentials, and Visual Hallucinations. *Journal of Neuroscience* **33**:10544-10551 https://doi.org/10.1523/JNEUROSCI.3007-12.2013
19. **Kraehenmann R,** Pokorny D, Vollenweider L, et al. (2017) Dreamlike effects of LSD on waking imagery in humans depend on serotonin 2A receptor activation. *Psychopharmacology (Berl)* **234**:2031-2046 https://doi.org/10.1007/s00213-017-4610-0
20. **Preller KH,** Herdener M, Pokorny T, et al. (2017) The Fabric of Meaning and Subjective Effects in LSD-Induced States Depend on Serotonin 2A Receptor Activation. *Curr Biol* **27** https://doi.org/10.1016/j.cub.2016.12.030
21. **Vollenweider F** (1997) Positron Emission Tomography and Fluorodeoxyglucose Studies of Metabolic Hyperfrontality and Psychopathology in the Psilocybin Model of Psychosis. *Neuropsychopharmacology* **16**:357-372 https://doi.org/10.1016/S0893-133X(96)00246-1
22. **Marek GJ** (2018) Interactions of hallucinogens with the glutamatergic system: Permissive network effects mediated through cortical layer V pyramidal neurons. In: Halberstadt AL, Vollenweider FX, Nichols DE (Eds). *Current Topics in Behavioral Neurosciences* **36** Springer Verlag. pp. 107-135

https://doi.org/10.1007/7854_2017_480

23. **Vargas M V.,** Dunlap LE, Dong C, et al. (2023) Psychedelics promote neuroplasticity through the activation of intracellular 5-HT2A receptors. *Science (1979)* **379**:700-706 https://doi.org/10.1126/science.adf0435
24. **de Vos CMH,** Mason NL, Kuypers KPC (2021) Psychedelics and Neuroplasticity: A Systematic Review Unraveling the Biological Underpinnings of Psychedelics. *Front Psychiatry* **12**:724606 https://doi.org/10.3389/fpsyt.2021.724606
25. **Ly C,** Greb AC, Cameron LP, et al. (2018) Psychedelics Promote Structural and Functional Neural Plasticity. *Cell Rep* **23**:3170-3182 https://doi.org/10.1016/j.celrep.2018.05.022
26. **Shao LX,** Liao C, Gregg I, et al. (2021) Psilocybin induces rapid and persistent growth of dendritic spines in frontal cortex in vivo. *Neuron* **109** https://doi.org/10.1016/j.neuron.2021.06.008
27. **Dakic V,** Minardi Nascimento J, Costa Sartore R, et al. (2017) Short term changes in the proteome of human cerebral organoids induced by 5-MeO-DMT. *Sci Rep* **7**:12863 https://doi.org/10.1038/s41598-017-12779-5
28. **Howe JR,** Bear MF, Golshani P, et al. (2018) The mouse as a model for neuropsychiatric drug development. *Current Biology* **28**:R909-R914 https://doi.org/10.1016/j.cub.2018.07.046
29. **Zahumenska R,** Nosal V, Smolar M, et al. (2020) Induced Pluripotency: A Powerful Tool for In Vitro Modeling. *Int J Mol Sci* **21**:8910 https://doi.org/10.3390/ijms21238910
30. **Chambers SM,** Fasano CA, Papapetrou EP, Tomishima M, Sadelain M, Studer L (2009) Highly efficient neural conversion of human ES and iPS cells by dual inhibition of SMAD signaling. https://doi.org/10.1038/nbt.1529
31. **Kemp PJ,** Rushton DJ, Yarova PL, et al. (2016) Improving and accelerating the differentiation and functional maturation of human stem cell-derived neurons: role of extracellular calcium and GABA. *J Physiol* **594**:6583-6594 https://doi.org/10.1113/JP270655
32. **Telezhkin V,** Schnell C, Yarova P, et al. (2016) Forced cell cycle exit and modulation of GABAA, CREB, and GSK3p signaling promote functional maturation of induced pluripotent stem cell- derived neurons. *American Journal of Physiology-Cell Physiology* **310**:C520-C541 https://doi.org/10.1152/ajpcell.00166.2015
33. **Sen A,** Hongpaisan J, Wang D, Nelson TJ, Alkon DL (2016) Protein Kinase Ce (PKCe) Promotes Synaptogenesis through Membrane Accumulation of the Postsynaptic Density Protein PSD-95. *Journal of Biological Chemistry* **291**:16462-16476 https://doi.org/10.1074/jbc.M116.730440
34. **Gray JA,** Roth BL (2001) Paradoxical trafficking and regulation of 5-HT(2A) receptors by agonists and antagonists. *Brain Res Bull* **56** https://doi.org/10.1016/s0361-9230(01)00623-2
35. **Raval NR,** Johansen A, Donovan LL, et al. (2021) A Single Dose of Psilocybin Increases Synaptic Density and Decreases 5-HT2A Receptor Density in the Pig Brain. *Int J Mol Sci* **22**:835 https://doi.org/10.3390/ijms22020835
36. **Colapo CS,** Alves SS, Nolli LM, et al. (2020) Toxicity of ayahuasca after 28 days daily exposure and effects on monoamines and brain-derived neurotrophic factor (BDNF) in brain of Wistar rats. *Metab Brain Dis* **35**:739-751 https://doi.org/10.1007/s11011-020-00547-w
37. **Almeida RN de,** Galvao AC de M, da Silva FS, et al. (2019) Modulation of Serum Brain-Derived Neurotrophic Factor by a Single Dose of Ayahuasca: Observation from a Randomized Controlled Trial. *Front Psychol* 10 https://doi.org/10.3389/fpsyg.2019.01234
38. **Inserra A,** Campanale A, Cheishvili D, et al. (2022) Modulation of DNA methylation and protein expression in the prefrontal cortex by repeated administration of D-lysergic acid diethylamide (LSD): Impact on neurotropic, neurotrophic, and neuroplasticity signaling. *Prog Neuropsychopharmacol Biol Psychiatry* **119**:110594 https://doi.org/10.1016/j.pnpbp.2022.110594
39. **De Gregorio D,** Inserra A, Enns JP, et al. (2022) Repeated lysergic acid diethylamide (LSD) reverses stress-induced anxiety-like behavior, cortical synaptogenesis deficits and serotonergic neurotransmission decline. *Neuropsychopharmacology* **47**:1188-1198

https://doi.org/10.1038/s41386-022-01301-9

40. **Lowe H,** Toyang N, Steele B, et al. (2021) The Therapeutic Potential of Psilocybin. *Molecules* **26**:2948 https://doi.org/10.3390/molecules26102948

41. **Kwan AC,** Olson DE, Preller KH, Roth BL (2022) The neural basis of psychedelic action. *Nat Neurosci* **25**:1407-1419 https://doi.org/10.1038/s41593-022-01177-4

42. **Berry SA,** Shah MC, Khan N, Roth BL (1996) Rapid agonist-induced internalization of the 5-hydroxytryptamine2A receptor occurs via the endosome pathway in vitro. *Mol Pharmacol* **50**

43. **Bhattacharyya S,** Puri S, Miledi R, Panicker MM (2002) Internalization and recycling of 5-HT 2A receptors activated by serotonin and protein kinase C-mediated mechanisms. *PNAS* **99**:14470-14475

44. **Kowianski P,** Lietzau G, Czuba E, Waskow M, Steliga A, Morys J (2018) BDNF: A Key Factor with Multipotent Impact on Brain Signaling and Synaptic Plasticity. *Cell Mol Neurobiol* **38**:579-593 https://doi.org/10.1007/s10571-017-0510-4

45. **Moliner R,** Girych M, Brunello CA, et al. (2023) Psychedelics promote plasticity by directly binding to BDNF receptor TrkB. *Nat Neurosci* **26**:1032-1041 https://doi.org/10.1038/s41593-023-01316-5

46. **de la Fuente Revenga M,** Zhu B, Guevara CA, et al. (2021) Prolonged epigenomic and synaptic plasticity alterations following single exposure to a psychedelic in mice. *Cell Rep* **37**:109836 https://doi.org/10.1016/j.celrep.2021.109836

47. **Wojtas A,** Bysiek A, Wawrzczak-Bargiela A, et al. (2022) Effect of Psilocybin and Ketamine on Brain Neurotransmitters, Glutamate Receptors, DNA and Rat Behavior. *Int J Mol Sci* **23**:6713 https://doi.org/10.3390/ijms23126713

48. **Mason NL,** Kuypers KPC, Müller F, et al. (2020) Me, myself, bye: regional alterations in glutamate and the experience of ego dissolution with psilocybin. *Neuropsychopharmacology* **45**:2003-2011 https://doi.org/10.1038/s41386-020-0718-8

49. **Muschamp JW,** Regina MJ, Hull EM, Winter JC, Rabin RA (2004) Lysergic acid diethylamide and [-]- 2,5-dimethoxy-4-methylamphetamine increase extracellular glutamate in rat prefrontal cortex. *Brain Res* **1023**:134-140 https://doi.org/10.1016/j.brainres.2004.07.044

50. **Scruggs JL,** Schmidt D, Deutch AY (2003) The hallucinogen 1-[2,5-dimethoxy-4-iodophenyl]-2-aminopropane (DOI) increases cortical extracellular glutamate levels in rats. *Neurosci Lett* **346**:137-140 https://doi.org/10.1016/S0304-3940(03)00547-0

51. **Duman RS,** Aghajanian GK, Sanacora G, Krystal JH (2016) Synaptic plasticity and depression: new insights from stress and rapid-acting antidepressants. *Nat Med* **22** https://doi.org/10.1038/nm.4050

52. **Vollenweider FX,** Kometer M (2010) The neurobiology of psychedelic drugs: implications for the treatment of mood disorders. *Nat Rev Neurosci* **11**:642-651 https://doi.org/10.1038/nrn2884

53. **Ehrlich I** (2004) Postsynaptic Density 95 controls AMPA Receptor Incorporation during Long-Term Potentiation and Experience-Driven Synaptic Plasticity. *Journal of Neuroscience* **24**:916-927 https://doi.org/10.1523/JNEUROSCI.4733-03.2004

54. **Opazo P,** Sainlos M, Choquet D (2012) Regulation of AMPA receptor surface diffusion by PSD-95 slots. *Curr Opin Neurobiol* **22**:453-460 https://doi.org/10.1016/j.conb.2011.10.010

55. **Chater TE,** Goda Y (2014) The role of AMPA receptors in postsynaptic mechanisms of synaptic plasticity. *Front Cell Neurosci* 8 https://doi.org/10.3389/fncel.2014.00401

56. **Liao C,** Dua AN, Wojtasiewicz C, Liston C, Kwan AC (2025) Structural neural plasticity evoked by rapid-acting antidepressant interventions. *Nat Rev Neurosci* **26**:101-114 https://doi.org/10.1038/s41583-024-00876-0

57. **Schmidt M** (2024) The Psychedelic Psilocin Fosters Neuroplasticity in IPSC-Derived Human Cortical Neurons.

Peer reviews

Reviewer #1 (Public review):

Summary:

This study reports the effects of psilocin on iPSC-derived human cortical neurons.

Strengths:

The characterization was comprehensive, involving immunohistochemistry of various markers, 5-HT2A receptors, BDNF, and TrkB, transcriptomics analyses, morphological determination, electrophysiology, and finally synaptic protein measurements. The results are in close agreement with prior work (PMID 29898390) on rat cultured cortical neurons. Nevertheless, there is value in confirming those earlier findings and furthermore to demonstrate the effects in human neurons, which are important for translation. The genetic, proteomics, and cell structure analyses used in this paper are its major strength. The study supports the value of using iPSC-derived human cortical neurons for drug development involving psychedelics-related compounds.

Weaknesses:

(1) Line 140: 5-HT2A receptor expression was found via immunocytochemistry to reside in the somatodendritic and axonal compartments. However, prior work from ex vivo tissue using electron microscopy has found predominantly 5-HT2A receptor expression in the somatodendritic compartment (PMID: 12535944). Was this antibody validated to be 5-HT2A receptor-specific? Can the authors reason why the discrepancy may arise, and if the axonal expression is specific to the cultured neurons?

(2) Line 143: It would be helpful to specify the dose of psilocin tested, and describe how this dose was chosen.

(3) Figure 1: The interpretation is that the differential internalization in the axonal and somatodendritic compartments is time-dependent. However, given that only one dose is tested, it is also possible that this reflects dose dependence, with the longer time exposure leading to higher dose exposure, so these variables are related. That is, if a higher dose is given, internalization may also be observed after 10 minutes in the dendritic compartment.

(4) Figure 3 & 4: What is the 'control' here? A more appropriate control for the 24 hours after psilocin application would be 24 hours after vehicle application. Here the authors are looking at before and after, but the factor of time elapsed and perturbation via application is not controlled for.

(5) The sample size was not clearly described. In the figure legend, N = the number of neurites is provided, but it is unclear how many cells have been analyzed, and then how many of those cells belong to the same culture. These are important sample size information that should be provided. Relatedly, statistical analyses should consider that the neurites from the same cells are not independent. If the neurites indeed come from the same cells, then the sample size is much smaller and a statistical analysis considering the nested nature of the data should be used.

Comments on revisions:

The authors performed substantial experiments to check validity of the HTR2A antibody for the revision. Briefly, they found that western blot shows a single band, abolished by a blocking peptide, in neural progenitors and iPSC-derived neurons, suggesting positive results. However, they also detected immunofluorescence signals in HEK293 and HeLa cells, which

do not express 5-HT2A receptors as scRNAseq analysis of these cells show complete absence of the transcript. Therefore the antibody has epitope-selective binding but also has some non-specific binding, precluding its use. The authors rightfully removed the data related to the antibody in the revised manuscript. The account is repeated here to highlight to anyone who may find the information helpful. Overall, the additional results added rigor to the study.

https://doi.org/10.7554/eLife.104006.2.sa2

Reviewer #2 (Public review):

In this article, Schmidt et al use iPSC-derived human cortical neurons to test the effects the psychedelic psilocin in different models of neuroplasticity.

Using human iPSC-derived cortical neurons, the authors test the expression of 5-HT2A and subcellular distribution, as well as the effect of different times of exposure to psilocin on 5-HT2A expression. The authors evaluated the effect of the 5-HT2 antagonist ketanserin, as well as the inhibition of dynamin-dependent endocytic pathways with dynasore. Gene expression and plasticity (structural and functional) was also evaluated after different times of exposure to psilocin.

In general, results are interesting since they use the iPSC to evaluate the potentially translationally relevant effects of psilocin (the active metabolite of the psychedelic psilocybin).

Comments on revisions:

The authors have addressed all of my previous concerns. A particular strength of the rebuttal is that the authors corroborated the lack of selectivity/specificity of the anti-5-HT2A antibody used in earlier versions of the manuscript.

https://doi.org/10.7554/eLife.104006.2.sa1

Author response:

The following is the authors' response to the original reviews.

> ***Reviewer #1:***
>
> *Comment 1: 5-HT2A Antibody Specificity*
>
> *Was this antibody validated to be 5-HT2A receptor-specific? Can the authors reason why the discrepancy may arise, and if the axonal expression is specific to the cultured neurons?*

We performed extensive validation of the anti-5-HT2A receptor antibody (Alomone #ASR-033), which is summarized in the accompanying Author response images:

Positive findings (Author response image 1c-e, Author response image 2a): (1) Western blot showed a single band at the expected molecular weight (~50 kDa) in neural progenitors and iPSCderived neurons. (2) The blocking peptide (#BLP-SR033) abolished Western blot bands and markedly reduced immunofluorescence signals in neurons, confirming epitope-specific binding.

Negative findings (Author response image 1a-b, Author response image 2a-b, Author response image 3): (1) We detected positive immunofluorescence signals in HEK293 and HeLa cells (Author response image 1a-b), which do not express 5-HT2AR. (2) Western blot also showed bands in HEK293 and HeLa cells (Author response image 2a-b). (3) Single-cell RNA-seq

analysis of HEK293T cells confirmed complete absence of *HTR2A* expression (Author response image 3a). (4) qPCR showed no detectable *HTR2A* transcripts in iPSCs or HeLa cells (Ct > 36), while neural progenitors and neurons showed clear expression (Author response image 3b). (5) siRNA knockdown experiments failed to produce a corresponding decrease in immunofluorescence or Western blot signals, despite reduced *HTR2A* transcript levels (data not shown).

BLAST analysis: Protein BLAST analysis of the 13-amino acid immunogenic peptide sequence identified the human 5-HT2A receptor as the top hit (9/13 amino acids overlap). However, shorter sequence similarities were also found with other proteins, including APPBP1 (6/9 amino acids), Immunoglobulin Heavy Chain (6/7 amino acids), and Interleukin31 receptor (6/8 amino acids). While these partial homologies do not provide a definitive mechanistic explanation for the observed off-target binding, they illustrate that the epitope sequence is not entirely unique to the 5-HT2A receptor.

Conclusion: While our validation confirmed epitope-specific binding (blocking peptide effective in neurons), the antibody clearly detects something in cells that demonstrably lack HTR2A gene expression. This indicates off-target binding to other proteins sharing the epitope sequence. We have therefore removed all antibody-based 5-HT2A receptor experiments from the revised manuscript. This includes the receptor internalization data from Figure 1. The remaining findings (BDNF upregulation, gene expression changes, morphological effects, electrophysiology) are supported by independent methods including pharmacological blockade with ketanserin.

> *Comment 2: Psilocin Dose Selection*
>
> *It would be helpful to specify the dose of psilocin tested, and describe how this dose was chosen.*

We used 10 µM psilocin based on: (1) The seminal study by Ly et al. (2018), which demonstrated neuroplasticity effects at this concentration in rat cortical neurons. (2) Our own dose-response experiments (Figure S2B) showing maximal BDNF increase at 10 µM compared to lower concentrations (10 nM, 100 nM, 1 µM). We have clarified this in the revised Methods section.

> *Comment 3: Dose vs. Time Dependence*
>
> *Given that only one dose is tested, it is also possible that this reflects dose dependence, with the longer time exposure leading to higher dose exposure.*

We agree that dose dependence cannot be excluded with our current experimental design. This point is now moot as we have removed the 5-HT2A receptor internalization experiments from the manuscript. Future studies in our group will address dose-dependent effects on other readouts.

> *Comment 4: Control Conditions*
>
> *What is the 'control' here? A more appropriate control would be 24 hours after vehicle application.*

The control condition is indeed a vehicle (DMSO) control collected at the same time point as the experimental condition (i.e., 24 hrs post-treatment). We have clarified this in the revised figure legends and Methods section to avoid confusion.

> *Comment 5: Sample Size Description*
>
> *The sample size was not clearly described. Statistical analyses should consider that neurites from the same cells are not independent.*

We have expanded the sample size descriptions in the figure legends. Analyses were performed using 5-10 microscope images per condition, with 15 ROIs per image, across at least two independent differentiations from two genetic backgrounds. Regarding independence: each neurite segment exists within a distinct microenvironment and can be considered an independent measurement unit, consistent with established practices in the field (Paul et al., 2021, CNS Neurosci Ther). We acknowledge this increases statistical power and have noted this in the Methods.

> ***Reviewer #2:***
>
> *Comment 1: 5-HT2A Antibody Validation*
>
> *Without validation (using for example knockdown techniques to decrease expression of 5HT2A), the experiments using this antibody should be excluded from the manuscript.*

We agree with this assessment. As detailed in our response to Reviewer 1 (Comment 1) and documented in the Response to Reviewer Figure, our extensive validation attempts—including siRNA knockdown—could not conclusively demonstrate antibody specificity. We have removed all antibody-based 5-HT2A receptor experiments from the revised manuscript.

> *Comment 2: Serotonin in Cell Media*
>
> *Did the authors evaluate whether 5-HT is present in the cell media?*

The cell culture media used in our experiments does not contain serotonin. We have explicitly stated this in the revised Methods section.

> *Comment 3: Statistical Analysis of Figure S1F*
>
> *Some of the datasets are not statistically analyzed, such as Figure S1F.*

Figure S1F related to the 5-HT2A receptor experiments and has been removed from the revised manuscript along with the associated data.

> *Comment 4: Translational Validity of Prolonged Exposure*
>
> *The authors continuously exposed cells to psilocin for hours or days. Since this is not the model of what occurs in vivo, the findings lack translational validity.*

We acknowledge this limitation. Most experiments (BDNF, gene expression, branching) were conducted 24–48 hrs after a brief 10-minute exposure, which better reflects the in vivo situation. Prolonged exposures (96 hrs) were used specifically for synaptogenesis experiments based on literature showing that repeated LSD administration enhances spine density (Inserra et al., 2022; De Gregorio et al., 2022). Our in vitro system lacks metabolizing enzymes and glial cells, which may introduce temporal biases. We have added a discussion of these limitations in the revised manuscript.

> *Comment 5: Ketanserin Effect on BDNF*
>
> *In Figure 2E, ketanserin by itself seems to reduce BDNF density. How do the authors conclude that ketanserin blocks psi-induced effects?*

We identified that one cell line (Ctrl 1) with inherently higher BDNF density was inadvertently excluded from the ketanserin-only condition. After removing Ctrl 1 from all conditions and reanalyzing, the difference between Ctrl and Ket alone is no longer significant. The significant difference between Psi+Ket and Ket alone demonstrate that psilocin exerts effects that ketanserin can block, consistent with 5-HT2A receptor mediation. The revised figure and statistical analysis are included in the updated manuscript.

> *Comment 6: mCherry Localization mCherry (Fig 4A) seems to be retained in the nucleus.*

The CamKII promoter drives expression of cytoplasmic mCherry, which fills the entire neuron including soma, dendrites, and axons. The apparent nuclear signal reflects mCherry accumulation in the soma, which surrounds the nucleus. The images clearly show mCherry extending into neurites, which was essential for our Sholl analysis of neuronal complexity.

> *Comment 7: Reference 36*
>
> *Reference 36 is a review article that does not mention psilocin.*

Our statement refers broadly to serotonergic psychedelics increasing neurotrophic factors. Reference 36 (Colaço et al., 2020) examines ayahuasca, which contains the serotonergic psychedelic DMT. We have revised the text to clarify this point.

> *Summary of Major Revisions*

(1) Removed all 5-HT2A receptor antibody-based experiments from Figure 1 and supplementary figures due to inconclusive specificity validation. An Author response image documenting our validation attempts is provided.

(2) Clarified control conditions (vehicle controls at matched time points) in figure legends.

(3) Expanded sample size descriptions in Methods and figure legends.

(4) Re-analyzed ketanserin experiments with consistent cell line inclusion.

(5) Added discussion of translational limitations.

(6) Added new Figure S5 summarizing proposed signaling pathways.

(7) Expanded discussion on the relevance of iPSC-derived neurons for drug development.

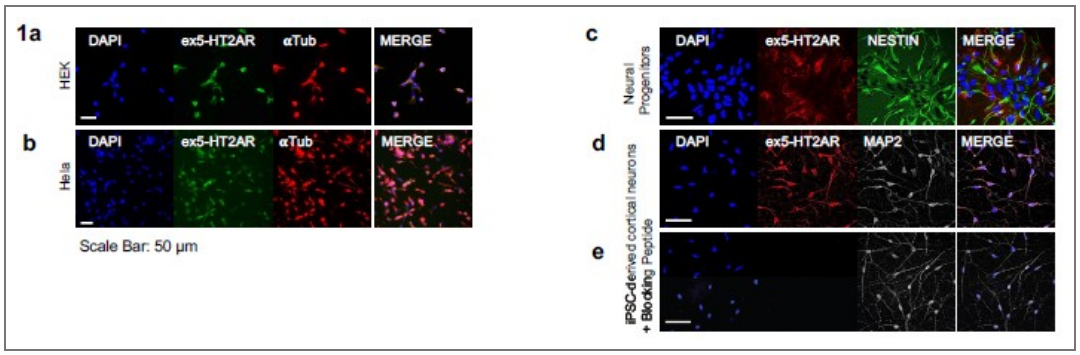

Author response image 1. Immunostaining for 5-HT2A receptor across cell types and peptide-blocking control. (a) HEK293 cells display a positive immunofluorescent signal despite not endogenously expressing 5-HT2AR, indicating nonspecific antibody reactivity. (b) HeLa cells also exhibit a positive signal despite lacking endogenous 5-HT2AR expression, further demonstrating nonspecific antibody binding in non-expressing cell types. (c) Neural progenitor cells show clear positive 5-HT2AR staining. (d) iPSC-derived neurons exhibit robust and well-defined 5-HT2AR staining. (e) Application of the Alomone 5-HT2AR blocking peptide (#BLP-SR033) markedly reduces neuronal signal intensity, supporting epitope-specific binding.

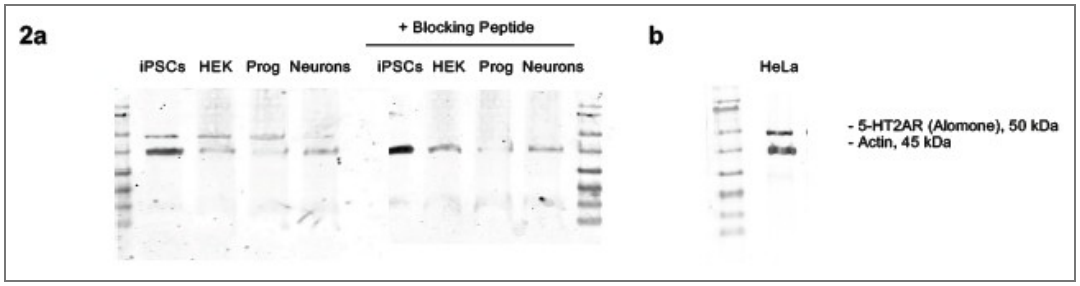

Author response image 2. Western blot analysis of 5-HT2A receptor abundance and peptide-blocking control. (a-b) In line with the immunofluorescence a single band is detected in iPSCs, HEK cells, neural progenitors, iPSC-derived neurons and (b) HeLa cells. (a) Preincubation of the primary antibody with the corresponding blocking peptide abolishes this band across all samples, consistent with specific binding of the antibody to its intended epitope.

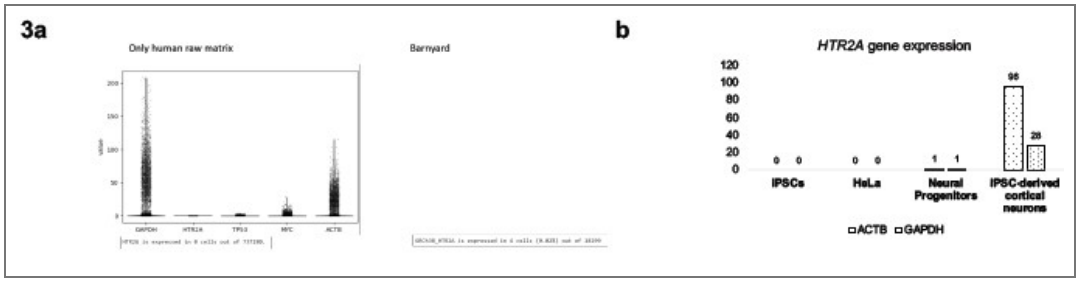

Author response image 3. Lack of detectable 5-HT2AR expression in HEK and HeLa cells. (a) Analysis of a human-only HEK293T single-cell RNA-seq dataset (10x Genomics; *https://www.10xgenomics.com/datasets/293-t-cells-1-standard-1-1-0*, accessed 2025-11-25) shows no meaningful *HTR2A* expression, whereas other genes such as *GAPDH*, *TP53*, *MYC*, and *ACTB* are robustly detected. Consistently, evaluation of a "Barnyard" dataset - an equal mixture of human HEK293T and mouse NIH3T3 cells (10x Genomics; *https://www.10xgenomics.com/datasets/20-k-1-1mixture-of-human-hek-293-t-and-mouse-nih-3-t-3-cells-3-ht-v-3-1-3-1-high-6-1-0*, accessed 2025-1125) reveals only ~4 of ~10,000 droplets with minimal HTR2A signal, confirming the absence of meaningful expression.(b) (b) qPCR analysis further demonstrates no detectable *HTR2A* transcripts in iPSCs or HeLa cells (Ct > 36), while neural progenitors and iPSC-derived cortical neurons show expression when normalized to housekeeping genes *GAPDH* and *TBP*.

https://doi.org/10.7554/eLife.104006.2.sa0